Spatial Variations of B-Value and Fundamental Parameters of The Earthquake Occurrences in The Eastern Mediterranean and Caucasus

Bahruz Ahadov (geofizik608@mail.ru)
Peking University https://orcid.org/0000-0002-4608-8138
Serkan Ozturk
Gumushane University: Gumushane Universitesi

Research Article

Keywords: Magnitude completeness(Mc), b-value, Stress variance, Hazard, Eastern Mediterranean, Caucasus

Posted Date: April 27th, 2021

DOI: https://doi.org/10.21203/rs.3.rs-321644/v1

Spatial variations of b-value and fundamental parameters of the earthquake occurrences in the Eastern Mediterranean and Caucasus

Bahruz Ahadov [1, 2, 3*] Serkan Ozturk[4]

[1] Shanghai Astronomical Observatory, Chinese Academy of Sciences, Shanghai 200030, China

[2] University of Chinese Academy of Sciences, Beijing 100049, China

[3]School of Earth and Space Sciences, Peking University, Beijing 100871, China

[4]Gümüşhane University, Department of Geophysics, TR-29100, Gümüşhane, Turkey

Email: geofizik608@mail.ru

Abstract

The Gutenberg-Richter (GR) law is a well-known empirical relation in seismology, which describes the frequency of earthquake occurrence as a function of the magnitude. The b-value anomalies may indicate the high or low-stress levels in the heterogeneity or the crust's thermal gradient. Some researchers have examined the spatial and temporal anomalies of the b-value before the mainshock and the aftershocks' spatial variability. The variations of the magnitude completeness (M_c) have estimated from the different earthquake catalogues. The high-resolution map of the GR b-value, M_c and stress variance have analysed in the different seismic regions in the Eastern Mediterranean and Caucasus. This study considered the spatial anomalies and correlation models between the b-value, faulting styles, and stress regime and moment release. Lower b-values ($b \leq 1$) were observed along with the Main Marmara Fault (MMF), eastern Turkey, western Alborz, northern Zagros, southeast Iran and the northeast Caucasus, which indicates the active seismic region. The M_c level in most of Turkey is in and around 2.8, and in the Caucasus is M_c=3, while Iran has M_c=3.5 value. This work includes a stress inversion map in the region based on the focal mechanisms. The normal, strike-slip and a few thrust fault solutions were observed in

the research area. Consequently, the spatial pattern of the b-values and stress regime can be used as a tool for predicting the forthcoming seismic hazard regions.

Keywords: Magnitude completeness (M_c) ; b -value; Stress variance; Hazard; Eastern Mediterranean; Caucasus.

1. Introduction

The Eastern Mediterranean and Caucasus are complex tectonic active regions associated with major lithospheric plates, Eurasian, Arabian, Nubia and Somalia (McKenzie, 1970; McKenzie, 1972) (Fig.1). The Eastern Mediterranean connected in the interaction zone of the Arabian, the Eurasian and Anatolian plates to the westward from the various intense convergence zone (Wdowinski et al., 2004). The plate motion includes thrust faults related to the Caucasus and the eastern Anatolian. The tectonic development of the region was formed by continental collision in the east of Turkey and subduction in Greece (Hellenic) (Jackson and McKenzie, 1984; Le Pichon and Angelier, 1979). The Anatolian block is placed among the African and Eurasian, and the Arabian plates since the collision (Jackson and McKenzie, 1984; McKenzie, 1972). The main tectonic settings of central Anatolian include intraplate pull basins and strike-slip faults. The North Anatolian Fault (NAF) describes the northern boundary with the Eurasian plateau, including a principal strike-slip fault (Barka and Kadinsky-Cade, 1988).

Previous studies have quantified regional deformation in interplay zone of the plate in the region (Ahadov and Jin, 2017, 2021; Aktuğ et al., 2013; Alchalbi et al., 2010; Mahmoud et al., 2005; McClusky et al., 2000; Meade et al., 2002). During history, the Mediterranean region has been hit by various destructive earthquakes. The seismicity of Turkey is different from Iran, as there are significant earthquakes in areas far from the three belts. Seismic activity in the western Anatolia was the most unusual geodynamic features in the region. There have been

large earthquakes with the magnitude of $Mw \geq 6$ due to historical seismic activity in the region (Table 1).

Many statistical studies have investigated the seismicity in distinct regions. (Mousavi, 2017b; Öztürk, 2015; Telesca et al. 2017; Öztürk, 2018). The seismic activity can present essential and reliable information about the stress concentration of earthquakes and Earth's formation in the region. The Mc value is an essential parameter for most questions related to seismicity. The M_c changes over time depending on the techniques of investigation and the number of seismic stations. The b-value can be implemented to evaluate the seismic hazard in a region to classify the stress. Therefore, the relationship between earthquakes and differences in the value of b is playing a role in earthquake prediction. High b-value is observed around volcanic chambers and while low b-value in the grooves section (Wiemer and Wyss, 2002). Many studies have noted that the value of b changes due to stress and heterogeneity in the crust (e.g. Khan and Chakraborty, 2007; Mogi, 1962; Mousavi, 2017b; Scholz, 1968; Wiemer and Katsumata, 1999; Wyss, 1973). The range of b-values between 0.3-2 has been published concerning tectonic events (Schorlemmer et al., 2005; Utsu, 1971). Earthquakes can be associated with energy release relevant to the fault dimensions, slip, and stress drop. The theory has been explained that measuring the magnitude of earthquake quantities and the results of the destruction (Kanamori, 1983).

The significance of this study is that the spatial model of b-value and seismotectonic features and their relation to tectonic settings in the Eastern Mediterranean and Caucasus have analysed. This study contributes a high-resolution map of the b-value between the released seismic moments, the fault mechanism, and the stress variability, which is the most relevant and integral part of seismicity. The conclusions can contribute significant constraints on crustal stress and hazard assessment in the region.

2. Data and Methods

The mapped b-value of the recurrence magnitude relationship of earthquakes from the background seismicity catalogues was based on Ml scale that was recorded by Kandilli Observatory, Earthquake Research Institute (KOERI, www.koeri.boun.edu.tr/sismo), International Seismological Centre (ISC, www.isc.ac.uk/iscbulletin) and International Institute of Earthquakes Engineering and Seismology (IIEES, www.iiees.ac.ir/en) from 1998 to 2020 ($M_l \geq 1$, Fig. 2) in the Turkey, Caucasus and Iran, respectively. In order to provide the frequency of earthquakes in the G-R relation, the first determined clusters and separate dependent events from the catalogues. The extent of earthquakes in the catalogue shows an almost linear increase over time. The relation between the amplitude of shock and the effects correlated with its existence called FMD, has been defined as (Gutenberg and Richter, 1944):

$$\log_{10} N(M) = a - bM \quad (1)$$

N is the number of events with a given magnitude M while a and b are constants, the constant a is related to the earthquake activity.

Wiemer and Wyss (1997) showed that low b-value along a fault zone corresponds to the features that regulate earthquake behaviour. Mc is determined at every grid node using the Best Combination approach (Wiemer, 2001) in the study region. The M_c value's standard deviation was achieved using the Bootstrapping process proposed by Schorlemmer et al., (2005).

The maximum likelihood relationship of G-R applied to calculate b-value, which has been observed more positive correlation with tectonic formations (Aki, 1965). Moreover, low stress has experienced in the seismogenic zone inducing episodic variations in the tectonic area (Wyss, 1973). The maximum likelihood approach provides a robust calculation of Mc in most cases and can be expressed as (Wiemer and Wyss, 1997):

$$\mathrm{b} = \frac{\log_{10}\mathrm{e}}{(\mathrm{M_{mean}} - \mathrm{M_{min}})} \quad (2)$$

M_{mean} is mean value of magnitude and M_{min} is the minimum rate of the completeness in the catalogues. The uncertainty of this assessment is provided by Eq. (3) as proposed by Shi and Bolt (1982):

$$\sigma(b) = 2.30b^2\sqrt{\sum_{i=1}^{n}(M_i - M_{mean})/n(n-1)} \quad (3)$$

where n is the complete number of events in the catalogue.

Earthquakes were collected from distinct catalogues and applied the corresponding interpolation technique (Wiemer and Wyss, 1997) to characterise the spatial accumulation value of b. The investigation is conducted on non-declustered and declustered catalogues. For each region, created a b-value map using the radius R_{max} = 80, 90, 140 km and determined b-value if at least R_{min}= 20, 15 and 15 events were available for individual grid node in Turkey, Caucasus and Iran, respectively. A bootstrap approach implemented to consider the reliability and quality of the b-value and Mc results. The number of events detected using $0.1^0 x 0.1^0$ grid node to compute the M_c and b-value, the density of data providing multiple events to be selected.

Different stress inversion techniques have been used to estimate the stress direction of the earthquake focal mechanism. Well-known methods of Gephart and Forsyth (1984) and Michael (1984) intend to determine the stress which minimizes the difference between the defined shear stress direction and the slip rate for a particular dataset. These algorithms explain the direction of the major stress arrows and the appropriate dimensions of stress, $R = (\sigma_2 - \sigma_3)/(\sigma_1 - \sigma_3)$. Here, $\sigma_1, \sigma_2, \sigma_3$ symbolises maximum, intermediate and minimum principal compressive stress, respectively.

In this study, stress inversion has produced using Michael's method. In a slick rule of Michael (Michael, 1984) the stress tensor is calculated applying a linear least-squares inversion technique. The algorithm uses each nodal planes to classify the fault plane while obtaining a particular stress tensor accurately. The algorithm's critical point is to determine the confidence threshold for the orientation of the principal stress arrows. Reliability thresholds have calculated by adopting a statistical tool known as bootstrap resampling. Maps of stress regime and variance have figured using six events per node with $0.2^0 x 0.2^0$ grid range.

In addition, estimated the seismic moment (M_0) from moment magnitude (M_w) to understand the stress accumulation by applying the standard relation from Kanamori and Brodsky (Kanamori and Brodsky, 2001),

$$LogM_0 = 1.5M_w + 9.1 \quad (4)$$

Different methods compute diverse scales of the magnitude and have other saturation states. We used an empirical relationship with additional references (Kadirioğlu and Kartal, 2016;

142 Mousavi-Bafrouei et al., 2015) to convert various magnitude scales (Ml to Mw) in each
143 database.

144

145 ## 3. Results and discussions

146 ### *3.1 Magnitude of completeness* (M_c)

147 The actual estimation rate of b-value depends on the completeness of the magnitude (M_c).
148 Mc is changing between time and space, with the earthquake catalogues and involves its
149 assessment. Evaluation of earthquake completeness catalogues is an essential step to learn in
150 all seismicity (Woessner and Wiemer, 2005). The variability of Mc depends on the seismic
151 activity and sensitivity of stations. The Mc is a fundamental parameter for all seismic
152 processing and may create an error while estimating the b-value because of the heterogeneity
153 of Mc values in the area. Since the study area is seismically active, Mc is estimated based on
154 the combined frequency-magnitude database. From the Mc map, it is seen that KOERI
155 catalogue in most of Turkey is resolved to Mc=2.8, in most of Caucasus the completeness level
156 is at Mc=3 from ISC catalogue, and in the IIEES catalogue of Iran it is Mc=3.5 (Fig.3). Most
157 of the areas were observed within the standard deviation of 0-0.1 in Iran and Turkey, while the
158 Caucasus is associated with higher errors ~ 0.3. Determination of *Mc*-value is desirable since
159 most applications demand many decisions when defining parameters such as seismicity rate or
160 b-values (Wiemer, 2001).

161 ### *3.2 b-value*

162 The value of b is considered correlated with developed heterogeneity of stress on the
163 crust (Mogi, 1962; Wiemer and Wyss, 1997) and a range of 0.5-1.5 (or with the error limits,
164 between 1.30 and 1.64) for tectonic earthquakes (Olsson, 1999). Several researchers (Mousavi
165 2017a; Öztürk 2011) have investigated spatial differences of b in the different seismic
166 regions. Öztürk (2011) evaluated seismic activity from several earthquake catalogues with an

167 average (~1) variations on diverse segments along the NAF. The map displays (Fig. 4 a, b) of
168 the calculated Mc and b-values from non-declustered and declustered catalogues using a
169 smaller radius with higher resolution. The epicentre of earthquakes is associated with low-
170 value areas ($b < 1$). The b-values are observed mainly less than one in Izmit, Erzurum and
171 Van. Low value ranges coincided by the spatial distribution in rupture area of earthquakes.
172 However, some cases have been considered in a good relationship between the b-values and
173 the rupture zone that occurred in 1999 the Izmit and in 2011 the Van earthquakes.

174 Mousavi (2017a) described the relationship between the moment release and b-value in
175 Iran between 2006-2016. The calculated values were observed between 0.8-1.5. Higher values
176 were observed in eastern and central Iran, while lower rates change in the northern Tabriz and
177 central Alborz. The calculated b-values of this study mainly ranged between 0.2-1.5 in Iran
178 (Fig. 5a, b). Due to significant tectonic stress and local variations on plate tectonic activity,
179 lower rates (below 1) observed in westernmost Kermanshah, southern Bam and eastward
180 Alborz. We see that larger values prevail in SSW Zagros, northern Kermanshah, and central
181 Iran. The value of b in the northwestern Alborz region and Mashhad is close to the hypothesis
182 that seismic energy falls for further severe earthquakes. The low value in the western
183 Kermanshah is reasonable to be a significant change in the Zagros region on the Iraqi-Iranian
184 border, has reported in the 2017 Sarpol-e Zahab earthquake. There are transparent connections
185 between high values from small earthquakes and dense fractures. Low values in some areas
186 indicate that mainly large-scale earthquakes were released energy.

187 The spatial mapping of the b value can investigate the seismotectonics of the region. A
188 recent study was used local network data by Telesca et al. (2017) found that higher values were
189 varied between 0.9-1.2 in the south and that lower value variation was observed in northern
190 Azerbaijan. In this study, the value of b estimated from different methods and data applying
191 declustered and non-declustered catalogues is more consistent with previous studies in a wide

192 area. The rates in the Caucasus generally range between 0.6-1.7. The current trends show that
193 higher values (1.3-1.6) in Armenia while lower values (below 0.8) were observed in Zaqatala,
194 Oghuz and Shamakhi along the MCTF in Azerbaijan (Fig. 6 a, b). Higher values may be
195 correlated with less intensive rocks that encounter inelastic failure at under stress levels.

196 Besides, the b -values were learned in depth (Fig. 7). The maximum value observed at a
197 depth of 14 km in Iran. We can also see that the low values ($b < 1$) were at 15-40 km and a
198 sharp increase at 33 km depth. A higher value was observed at a depth of 6 km in Turkey. The
199 sharp variations between ~ 1.1 and 1.6 are also present in the Caucasus at a depth of 12 km.
200 The depth of b value gives us a model of stress accumulation at different depths.

201 Fig. 8 describes that the b-values are extending from 0.6 to 2 along the main faults. The
202 profile (C-C') shows the highest values at a depth of 20-25 km along the EAF. When high
203 values are loaded with cracks, the response to the existing fault cracks reduces large
204 earthquakes due to the collapse (Wiemer and Wyss, 2000). An impressive observation involves
205 low-value areas in the southern Bitlis-Zagros and the eastward Greater Caucasus, indicating
206 high stress in the area. The low value was seen along the Marmara (E-E') at 20 km. A lower
207 value in the seismogenic zone has been agreed with a significant reduction in stress levels
208 before the mainshock (Kanamori, 1981).

209 *3.3 Stress Tensor Inversion*

210 In this study, a total of 1020 Focal Mechanism Solutions were selected from the Global
211 Centroid Moment Tensor database. The spatial occurrence of earthquakes suggests that the
212 data has sufficient resolution to indicate the stress regime and measure the variability in the
213 region. The distribution of the earthquakes is linked to the combination of existing faults, and
214 these mechanisms are compatible with the understanding of changes along the faults. The b-
215 values usually vary with the source mechanism of the earthquakes. The highest values confirm

normal fault events, average values indicate strike-slip events, and the lowest values show thrusts events, respectively (Schorlemmer et al., 2005). Fig. 9 reveals the colour bars displaying horizontal compression directions and associated tectonic structures. In addition to normal faults, some areas have a complex strike-slip fault, such as western Anatolian, some parts of the Caspian Sea and south-eastern Iran. The low b-values indicate regions, including strike and inverse slip faults corresponding to the features of the tectonic zone. It is an essential consequence of b closer to a low value in Turkey, the Great Caucasus, Zagros, Kopet-Dagh and eastern Alborz. These zones are associated with the thrust and strike-slip faulting, which is under a higher stress regime. Stress variability in the region is also different in several areas (Fig. 10). The stress variance is completely under this limit except for the confined area of the study region. The variation map shows that highly variable areas overlap with high b-values and correlates with low-stress variability and where the variance is less than 0.2. The stress difference is more than 0.2 means a different stress area or a decreased resolution of data.

3.4 Comparison with seismic moment release

Most of the area leads to a correlation between the b-value and the seismic moment's release. The seismic moment release (Fig.11) was calculated on each grid node with an interval of $0.5^0 x 0.5^0$ and compared with the b-value map. A lower value variation and higher moment release were observed in Izmit, Van and Erzurum, which indicates the location of high-stress zones. The Eastern Caucasus have intermediate value changes with an average moment release. The observation shows a lower b-value (~0.7) and high seismic moment rate (~18) on the Bitlis-Zagros thrust belt.

4. Conclusion

In this study, the spatial changes of the b-value were evaluated by analysing earthquake events within 1998-2020 years from the different catalogues such as the ISC, KOERI and IIEES. The investigation of seismicity is essential for evaluating seismic hazards and a better understanding of the different tectonic features in the seismogenic zone. The estimated completeness of the magnitude level is 2.8 in most of Turkey, M_c=3 in the Caucasus, and it was observed 3.5 in Iran. b-value was investigated by the time and space up to a wide variety of long-term and different earthquake catalogues. Obtained results from the non-declustered and declustered catalogues are better correlated with other b-value studies in the geodynamics and structure of the region. Higher values were found in the western Turkey, eastern and central Iran and the south western Caucasus. In certain areas, lower values were associated with extensive faulting result in low heterogeneity and large earthquakes. The b-value is not only indicated the relative size of small and large earthquakes also related to the stress state over the region. The b-values characterised the earthquakes and stayed around one. Therefore, it may be assumed that most of the region is low value and seismically active. Completed results are coherent with the tectonic formation of the area when the overall region was considered. Mainly strike-slip movements and the principal stress directions support the adjustment of the focal mechanisms. The low and medium b-values in the region are under the impact of the tectonic process from the African, Arabian and Eurasian Plates presented by the strike and thrust slip deformations. The b-value mapping is a relevant tool for displaying different levels of stress across large areas. As a result, a massive earthquake has occurred in the high-stress areas (low-value), and there was no significant earthquake in the high-value areas. Therefore, spatial maps of the b-values and stress mode maps can be appropriated as a tool for consequent seismic hazard and earthquake zones.

Acknowledgement

All the maps are drawn using Generic Mapping Tools (GMT) (Wessel et al., 2013), and the graphs are plotted using ZMAP (Wiemer, 2001). This research did not receive any specific grant from funding agencies in the public, commercial, or not-for-profit sectors.

Conflicts of interest/Competing interests

The authors declare no conflict of interest.

Ethics approval

Authors are responsible for the reliability of the manuscript and collaborate with the Editorial Office when original pictures and data, and other proof materials are required.

References

Ahadov, B., Jin, S., 2017. Present-day kinematics in the Eastern Mediterranean and Caucasus from dense GPS observations. Physics of the Earth and Planetary Interiors 268, 54-64.

Ahadov, B. and Jin, S., 2021. Slip Rates and Seismic Potential Along Main Faults in the Eastern Mediterranean and Caucasus from dense GPS Observations and Seismic Data. *Pure and Applied Geophysics*, pp.1-16.

Aki, K., 1965. Maximum likelihood estimate of b in the formula log N=a-bM and its confidence limits. Bull. Earthq. Res. Inst., Tokyo Univ. 43, 237-239.

Aktuğ, B., Parmaksız, E., Kurt, M., Lenk, O., Kılıçoğlu, A., Gürdal, M.A., Özdemir, S., 2013. Deformation of Central Anatolia: GPS implications. Journal of Geodynamics 67, 78-96.

Alchalbi, A., Daoud, M., Gomez, F., McClusky, S., Reilinger, R., Romeyeh, M.A., Alsouod, A., Yassminh, R., Ballani, B., Darawcheh, R., 2010. Crustal deformation in northwestern Arabia from GPS measurements in Syria: Slow slip rate along the northern Dead Sea Fault. Geophysical Journal International 180, 125-135.

289 Barka, A., Kadinsky-Cade, K., 1988. Strike-slip fault geometry in Turkey and its influence on
290 earthquake activity. Tectonics 7, 663-684.
291 Gephart, J.W., Forsyth, D.W., 1984. An improved method for determining the regional stress
292 tensor using earthquake focal mechanism data: application to the San Fernando earthquake
293 sequence. Journal of Geophysical Research: Solid Earth 89, 9305-9320.
294 Gutenberg, B., Richter, C.F., 1944. Frequency of earthquakes in California. Bulletin of the
295 Seismological Society of America 34, 185-188.
296 Jackson, J., McKenzie, D., 1984. Active tectonics of the Alpine–Himalayan Belt between
297 western Turkey and Pakistan. Geophysical Journal International 77, 185-264.
298 Kadirioğlu, F.T., Kartal, R.F., 2016. The new empirical magnitude conversion relations using
299 an improved earthquake catalogue for Turkey and its near vicinity (1900-2012). Turkish
300 Journal of Earth Sciences 25, 300-310.
301 Kamer, Y., Hiemer, S., 2015. Data-driven spatial b value estimation with applications to
302 California seismicity: To b or not to b. Journal of Geophysical Research: Solid Earth 120, 5191-
303 5214.
304 Kanamori, H., 1981. The nature of seismicity patterns before large earthquakes.
305 Kanamori, H., 1983. Magnitude scale and quantification of earthquakes. Tectonophysics 93,
306 185-199.
307 Kanamori, H., Brodsky, E.E., 2001. The physics of earthquakes. Physics Today 54, 34-40.
308 Khan, P., Chakraborty, P.P., 2007. The seismic b-value and its correlation with Bouguer gravity
309 anomaly over the Shillong Plateau area: tectonic implications. Journal of Asian Earth Sciences
310 29, 136-147.
311 Le Pichon, X., Angelier, J., 1979. The Hellenic arc and trench system: a key to the neotectonic
312 evolution of the eastern Mediterranean area. Tectonophysics 60, 1-42.

313 Mahmoud, S., Reilinger, R., McClusky, S., Vernant, P., Tealeb, A., 2005. GPS evidence for
314 northward motion of the Sinai Block: implications for E. Mediterranean tectonics. Earth and
315 Planetary Science Letters 238, 217-224.
316 McClusky, S., Balassanian, S., Barka, A., Demir, C., Ergintav, S., Georgiev, I., Gurkan, O.,
317 Hamburger, M., Hurst, K., Kahle, H., 2000. Global Positioning System constraints on plate
318 kinematics and dynamics in the eastern Mediterranean and Caucasus. Journal of Geophysical
319 Research: Solid Earth 105, 5695-5719.
320 McKenzie, D., 1970. Plate tectonics of the Mediterranean region. Nature 226, 239-243.
321 McKenzie, D., 1972. Active Tectonics of the Mediterranean Region. Geophysical Journal
322 International 30, 109-185.
323 Meade, B.J., Hager, B.H., McClusky, S.C., Reilinger, R.E., Ergintav, S., Lenk, O., Barka, A.,
324 Özener, H., 2002. Estimates of seismic potential in the Marmara Sea region from block models
325 of secular deformation constrained by Global Positioning System measurements. Bulletin of
326 the Seismological Society of America 92, 208-215.
327 Michael, A.J., 1984. Determination of stress from slip data: faults and folds. Journal of
328 Geophysical Research: Solid Earth 89, 11517-11526.
329 Mogi, K., 1962. Magnitude-frequency relation for elastic shocks accompanying fractures of
330 various materials and some related problems in earthquakes. Bull. Earthq. Res. Inst., Univ.
331 Tokyo 40, 831-853.
332 Mousavi-Bafrouei, S.H., Mirzaei, N., Shabani, E., 2015. A declustered earthquake catalog for
333 the Iranian Plateau. Annals of Geophysics 57.
334 Mousavi, S.M., 2017a. Mapping seismic moment and b-value within the continental-collision
335 orogenic-belt region of the Iranian Plateau. Journal of Geodynamics 103, 26-41.

336 Mousavi, S.M., 2017b. Spatial variation in the frequency-magnitude distribution of
337 earthquakes under the tectonic framework in the Middle East. Journal of Asian Earth Sciences
338 147, 193-209.
339 Olsson, R., 1999. An estimation of the maximum *b*-value in the Gutenberg-Richter relation.
340 Geodynamics, 27, 547–552.
341 Öztürk, S., 2011. Characteristics of seismic activity in the Western, Central and Eastern parts
342 of the North Anatolian Fault Zone, Turkey: Temporal and spatial analysis. Acta Geophysica
343 59, 209-238.
344 Öztürk, S., 2015. A study on the correlations between seismotectonic b-value and Dcvalue, and
345 seismic quiescence Z-value in the Western Anatolian region of Turkey. Austrian Journal of
346 Earth Sciences 108.
347 Öztürk, S., 2018. Earthquake hazard potential in the Eastern Anatolian Region of Turkey:
348 seismotectonic b and Dc-values and precursory quiescence Z-value. Frontiers of earth science
349 12, 215-236.
350 Scholz, C., 1968. The frequency-magnitude relation of microfracturing in rock and its relation
351 to earthquakes. Bulletin of the seismological society of America 58, 399-415.
352 Schorlemmer, D., Wiemer, S., Wyss, M., 2005. Variations in earthquake-size distribution
353 across different stress regimes. Nature 437, 539.
354 Shi, Y., Bolt, B.A., 1982. The standard error of the magnitude-frequency b value. Bulletin of
355 the Seismological Society of America 72, 1677-1687.
356 Telesca, L., Kadirov, F., Yetirmishli, G., Safarov, R., Babayev, G. and Ismaylova, S., 2017.
357 Statistical analysis of the 2003–2016 seismicity of Azerbaijan and surrounding areas. *Journal*
358 *of Seismology*, *21*(6), pp.1467-1485.

359 Utsu, T., 1971. Aftershocks and earthquake statistics (2): further investigation of aftershocks
360 and other earthquake sequences based on a new classification of earthquake sequences. Journal
361 of the Faculty of Science, Hokkaido University. Series 7, Geophysics 3, 197-266.
362 Wdowinski, S., Bock, Y., Baer, G., Prawirodirdjo, L., Bechor, N., Naaman, S., Knafo, R.,
363 Forrai, Y., Melzer, Y., 2004. GPS measurements of current crustal movements along the Dead
364 Sea Fault. Journal of Geophysical Research: Solid Earth 109.
365 Wessel, P., Smith, W.H., Scharroo, R., Luis, J., Wobbe, F., 2013. Generic mapping tools:
366 improved version released. Eos, Transactions American Geophysical Union 94, 409-410.
367 Wiemer, S., 2001. A software package to analyze seismicity: ZMAP. Seismological Research
368 Letters 72, 373-382.
369 Wiemer, S., Katsumata, K., 1999. Spatial variability of seismicity parameters in aftershock
370 zones. Journal of Geophysical Research: Solid Earth 104, 13135-13151.
371 Wiemer, S., Wyss, M., 1997. Mapping the frequency-magnitude distribution in asperities: An
372 improved technique to calculate recurrence times? Journal of Geophysical Research: Solid
373 Earth 102, 15115-15128.
374 Wiemer, S., Wyss, M., 2000. Minimum magnitude of completeness in earthquake catalogs:
375 Examples from Alaska, the western United States, and Japan. Bulletin of the Seismological
376 Society of America 90, 859-869.
377 Wiemer, S., Wyss, M., 2002. Mapping spatial variability of the frequency-magnitude
378 distribution of earthquakes, Advances in geophysics. Elsevier, pp. 259-V.
379 Woessner, J., Wiemer, S., 2005. Assessing the quality of earthquake catalogues: Estimating
380 the magnitude of completeness and its uncertainty. Bulletin of the Seismological Society of
381 America 95, 684-698.
382 Wyss, M., 1973. Towards a physical understanding of the earthquake frequency distribution.
383 Geophysical Journal International 31, 341-359.

Fig. 1 Tectonic and topographic/bathymetric map (SRTM30 plus) of the research area, including the interplay zone of the Eurasian, Arabian and Nubia plates. Abbreviations: AG (Aegean), NAF (North Anatolian Fault), EAF (East Anatolian Fault), DSTF (Dead Sea Transform Fault), NEAF (North-East Anatolian Fault), CF (Chalderan Fault), NTF (North Tabriz Fault). Black beach balls represent the focal mechanism of the earthquakes ($\boldsymbol{M_w \geq 5.5}$, 1976-2020) from global Centroid Moment Tensor CMT).

Fig. 2 The map represents the distribution of the earthquakes in the study region (1998-2020).

Fig. 3 Frequency-magnitude number of earthquakes from. The solid line and triangle marked as best fit and magnitude of completeness.

Fig. 4 The maps of calculated b-value and *Mc* variations from non-declustered (upper) and declustered (bottom) catalogues for Turkey in the period of 1998-2020 from KOERI catalogue.

Fig. 5 The maps of calculated b-value and *Mc* variations from non-declustered (upper) and declustered (bottom) catalogues in the period 1998-2020 for Iran using IIEES catalogue.

Fig. 6 The maps of calculated b-value and *Mc* variations from non-declustered (upper) and declustered (bottom) catalogues in the period 1998-2020 in the Caucasus.

Fig. 7 The map shows the calculated value of b and its error (horizontal bar) at a depth.

Fig. 8 Vertical mapping of b-values. The left line shows the intersections. In the middle line, a b-value of 150 km is given around each section. In the right line, the pattern of b-value is presented.

Figure 9 The direction of horizontal compression, different colors symbolize tectonic modes. (NF: Normal, NS: Normal with strike-slip, SS: Strike-slip, TS: Thrust with strike-slip, TF: Thrust).

Fig. 10 Horizontal compression orientation covered colored stress tensor variance map.

Fig. 11 The map shows estimated moment release from the different catalogues from 1998 to 2020.

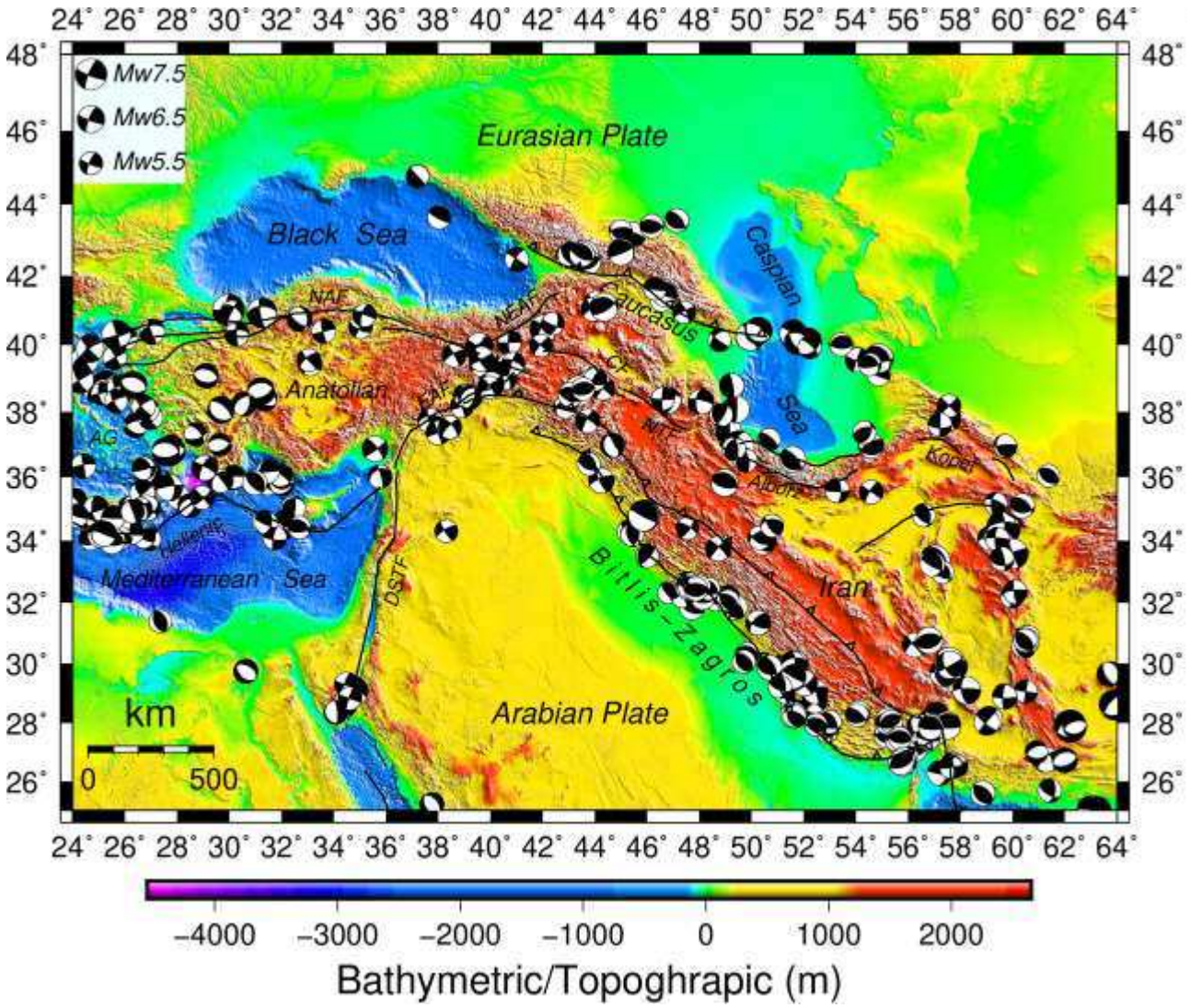

Fig. 1 Tectonic and topographic/bathymetric map (SRTM30 plus) of the research area, including the interplay zone of the Eurasian, Arabian and Nubia plates. Abbreviations: AG (Aegean), NAF (North Anatolian Fault), EAF (East Anatolian Fault), DSTF (Dead Sea Transform Fault), NEAF (North-East Anatolian Fault), CF (Chalderan Fault), NTF (North Tabriz Fault). Black beach balls represent the focal mechanism of the earthquakes ($\boldsymbol{M_w \geq 5.5}$, 1976-2020) from global Centroid Moment Tensor CMT).

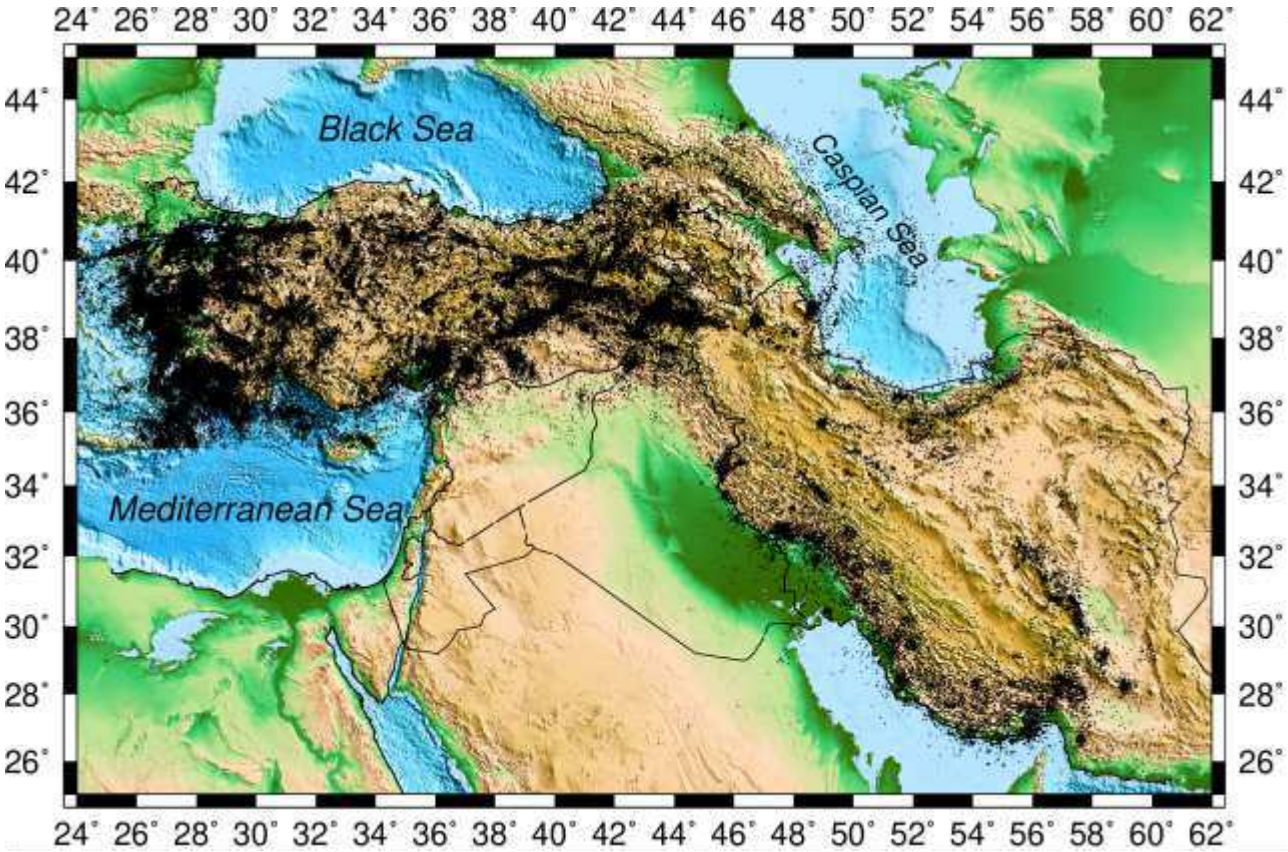

Fig. 2 The map represents the distribution of the earthquakes in the study region (1998-2020).

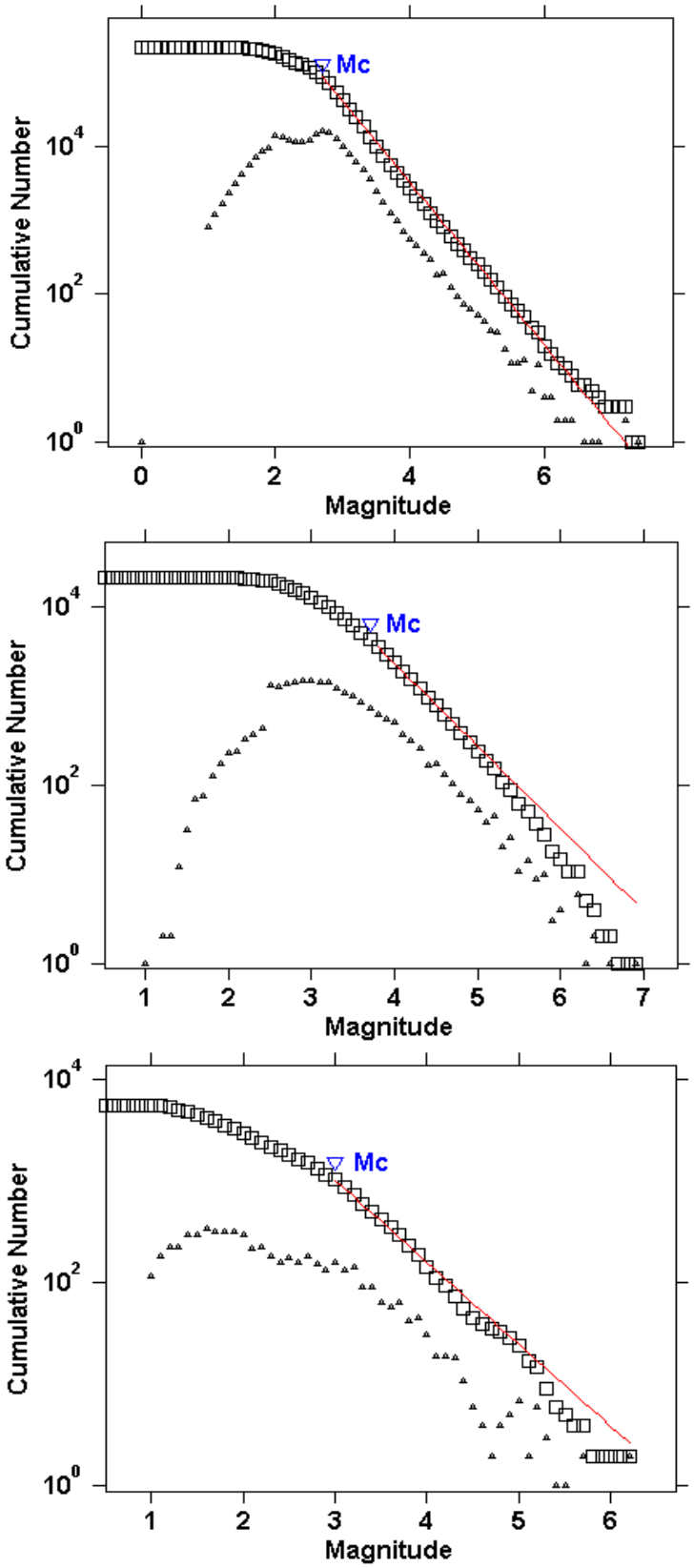

Fig. 3 Frequency-magnitude number of earthquakes from. The solid line and triangle marked as best fit and magnitude of completeness.

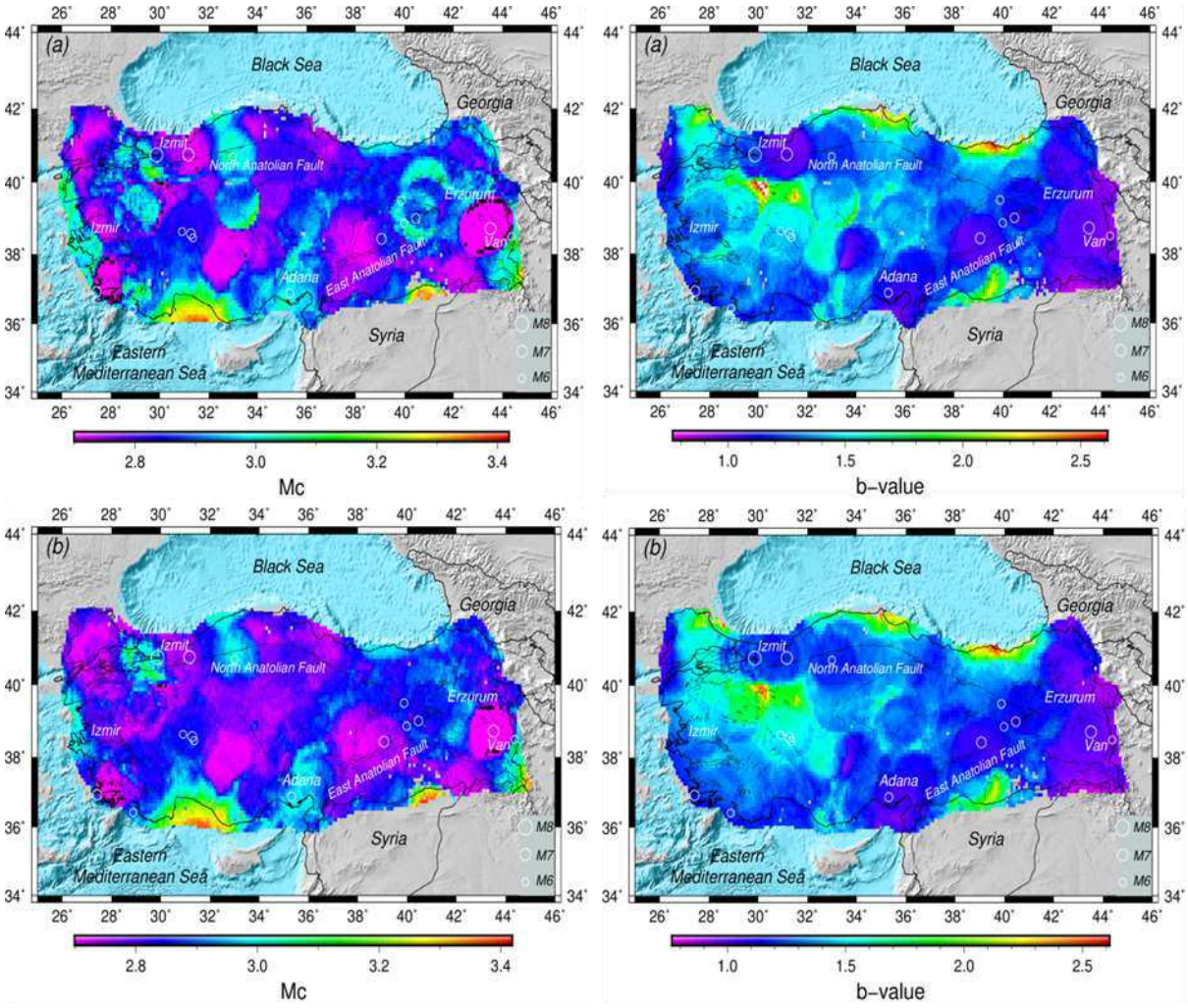

Fig. 4 The maps of calculated *b*-value and *Mc* variations from non-declustered (upper) and declustered (bottom) catalogues for Turkey in the period of 1998-2020 from KOERI catalogue.

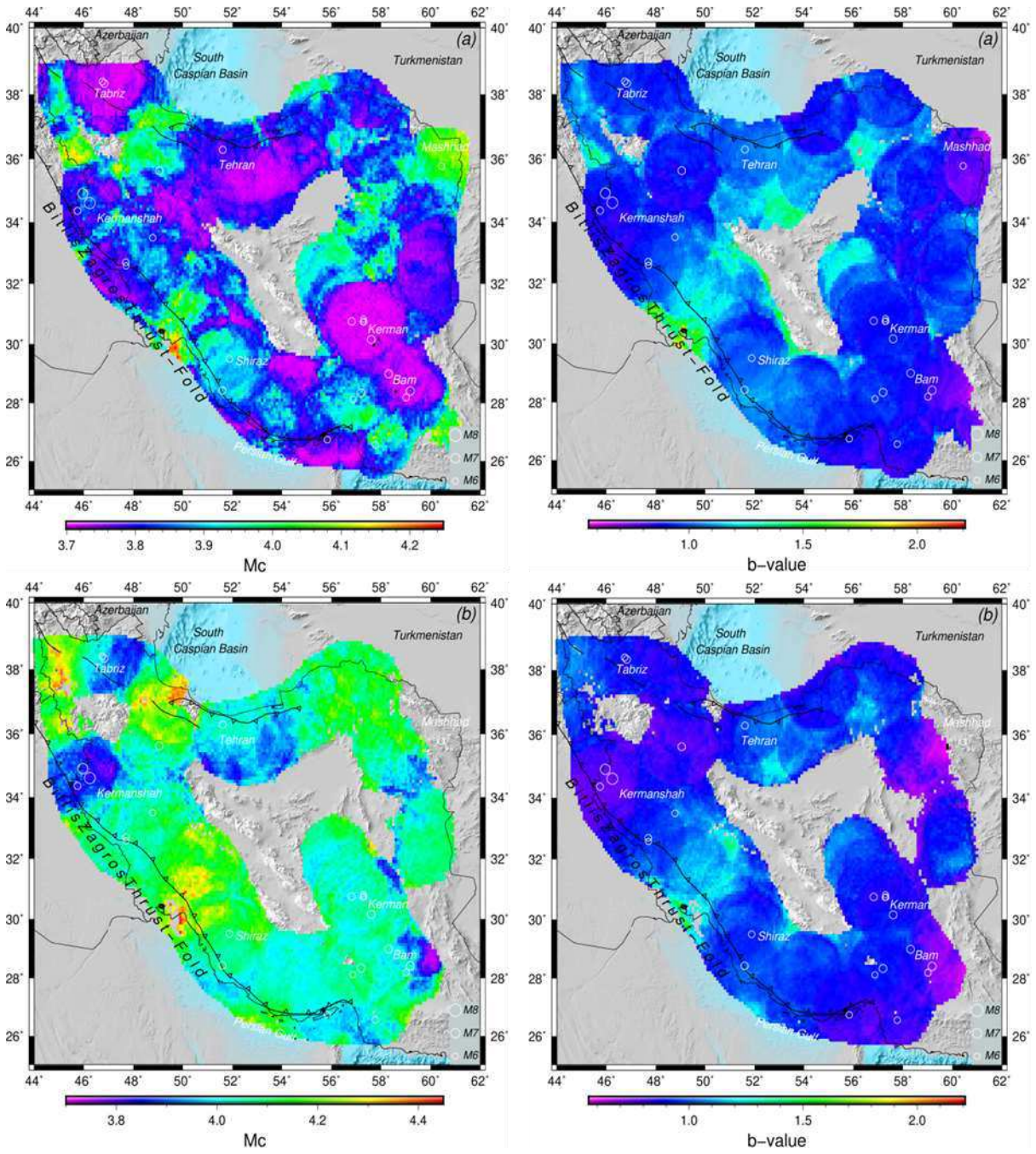

Fig. 5 The maps of calculated *b*-value and *Mc* variations from non-declustered (upper) and declustered (bottom) catalogues in the period 1998-2020 for Iran using IIEES catalogue.

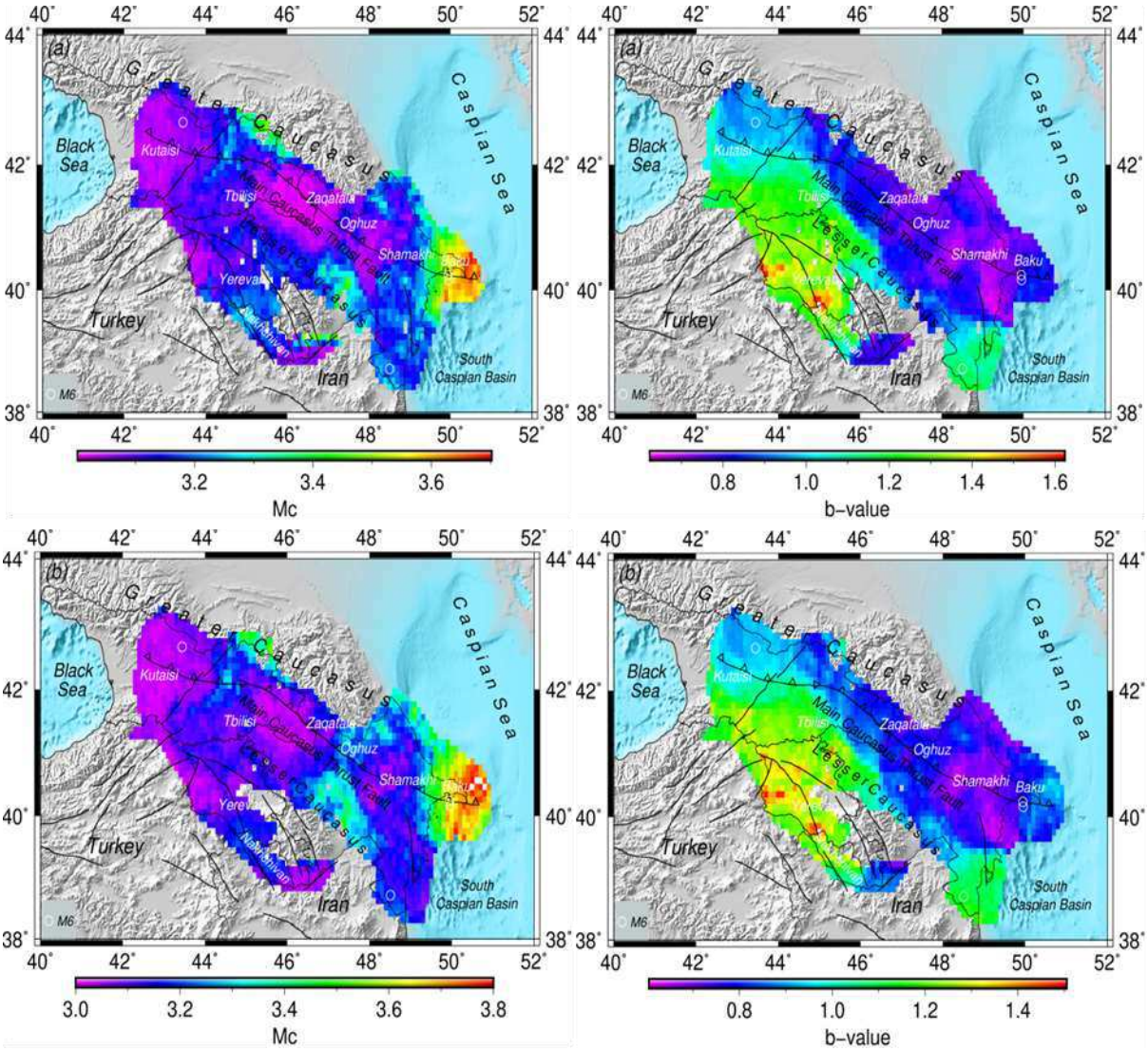

452

453 **Fig. 6** The maps of calculated *b*-value and *Mc* variations from non-declustered (upper) and
454 declustered (bottom) catalogues in the period 1998-2020 in the Caucasus

455

456

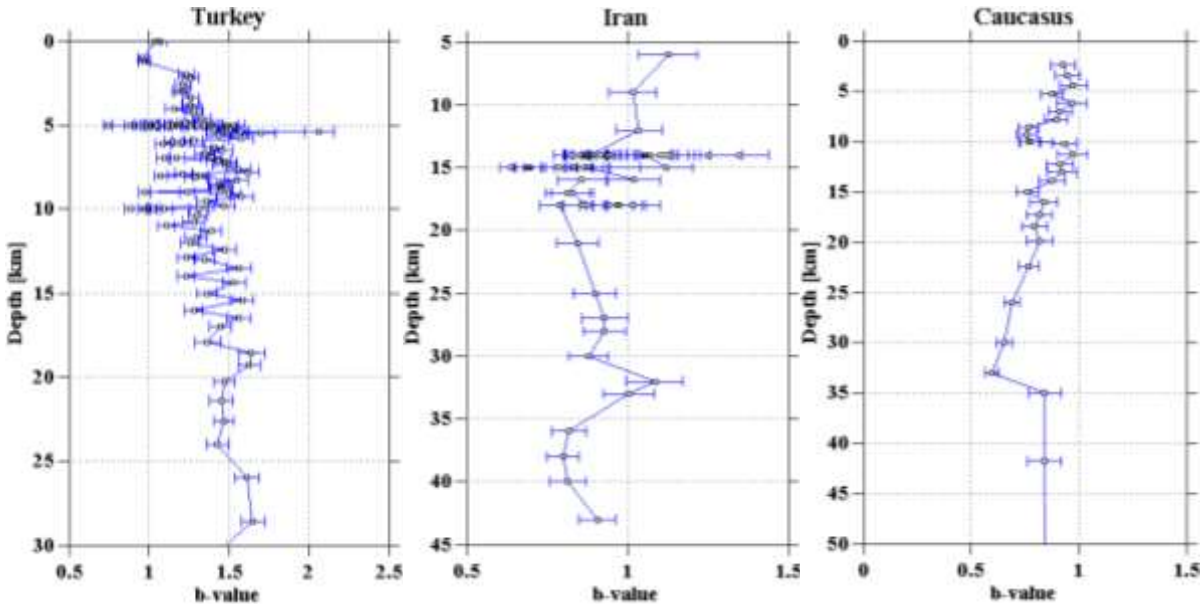

Fig. 7 The map shows the calculated value of *b* and its error (horizontal bar) at a depth

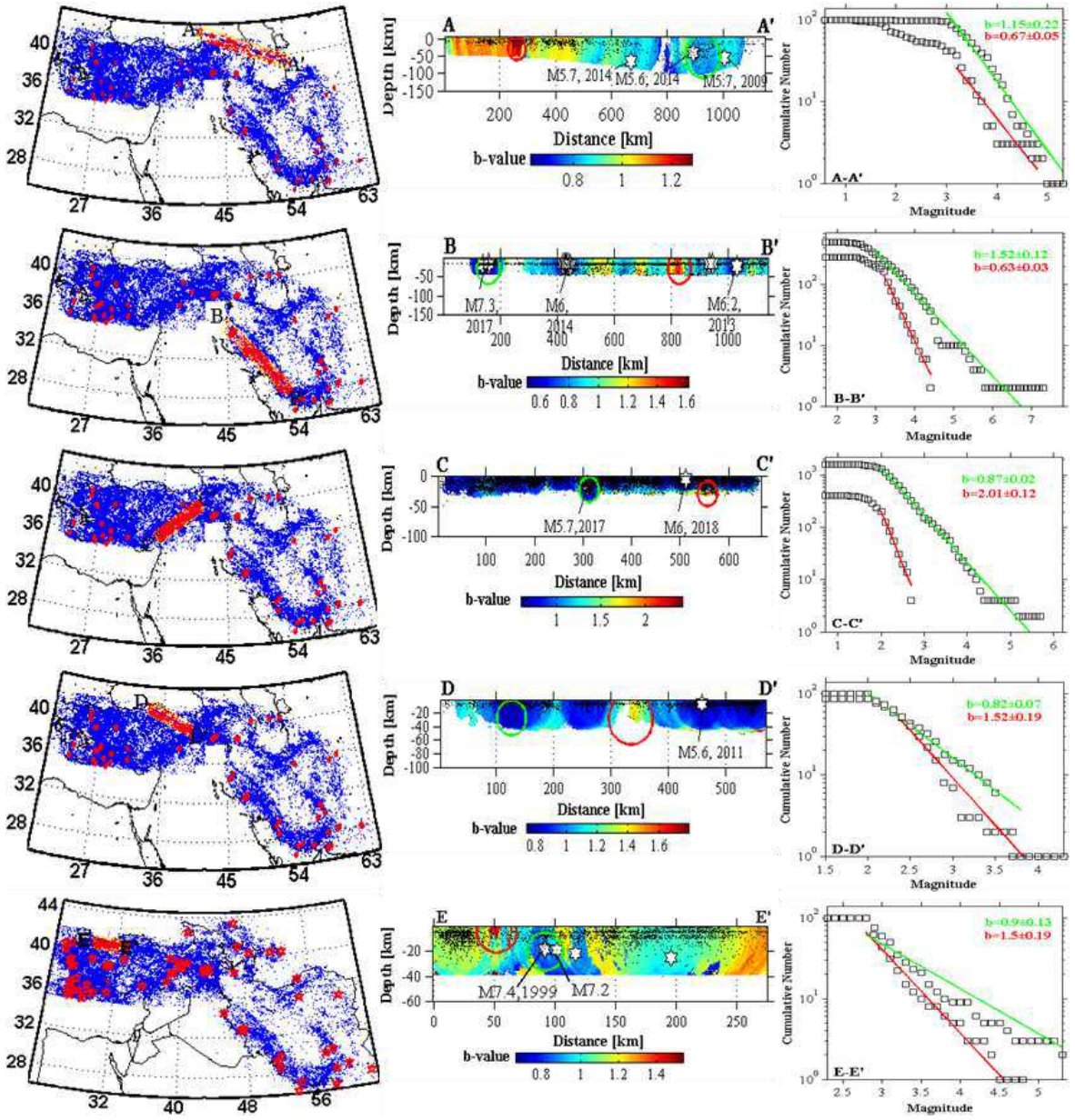

Fig. 8 Vertical mapping of *b*-values. The left line shows the intersections. In the middle line, a *b*-value of 150 km is given around each section. In the right line, the pattern of *b*-value is presented.

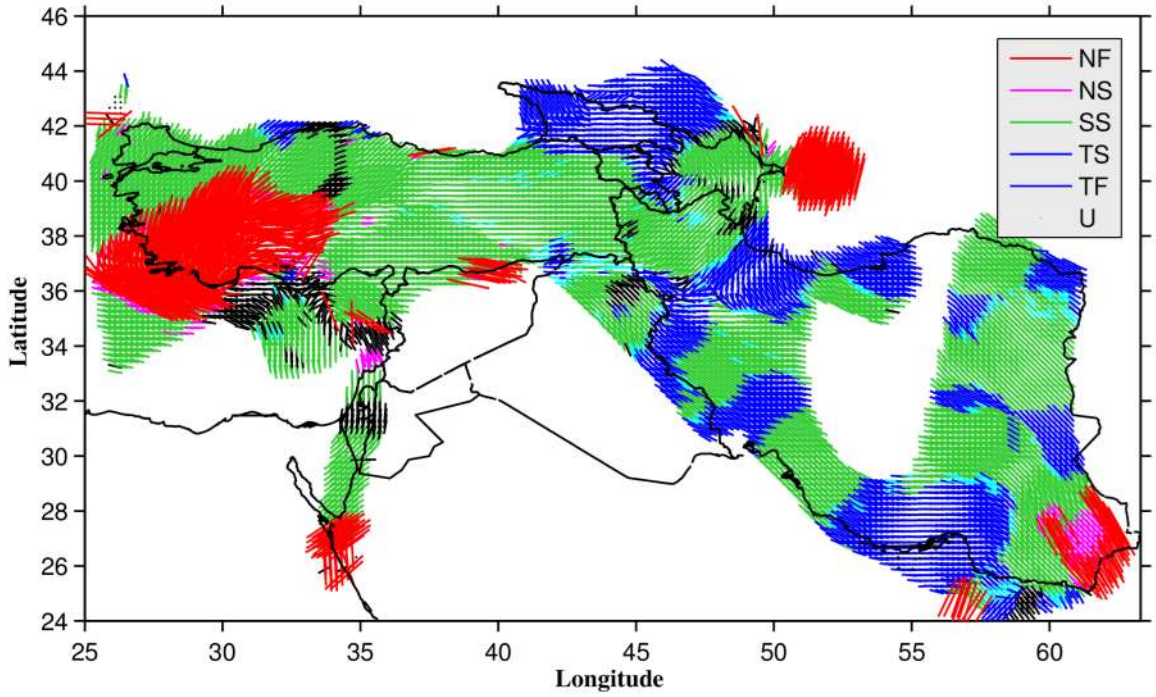

Fig. 9 The direction of horizontal compression, different colors symbolize tectonic modes. (NF: Normal, NS: Normal with strike-slip, SS: Strike-slip, TS: Thrust with strike-slip, TF: Thrust).

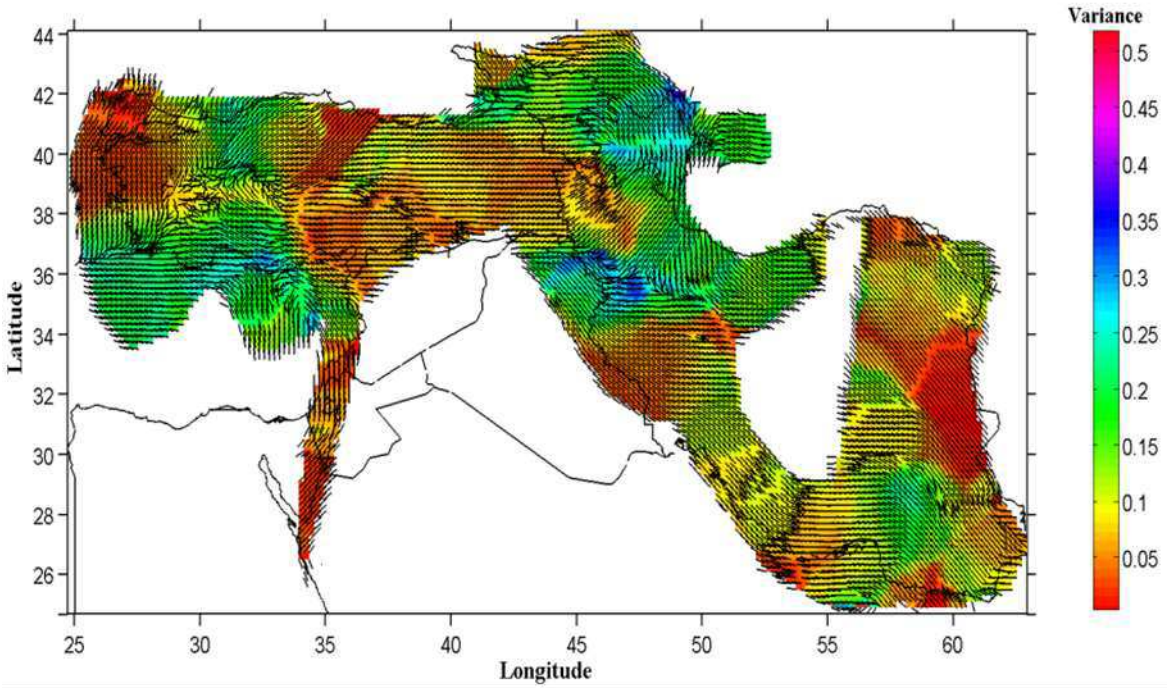

Fig. 10 Horizontal compression orientation covered colored stress tensor variance map.

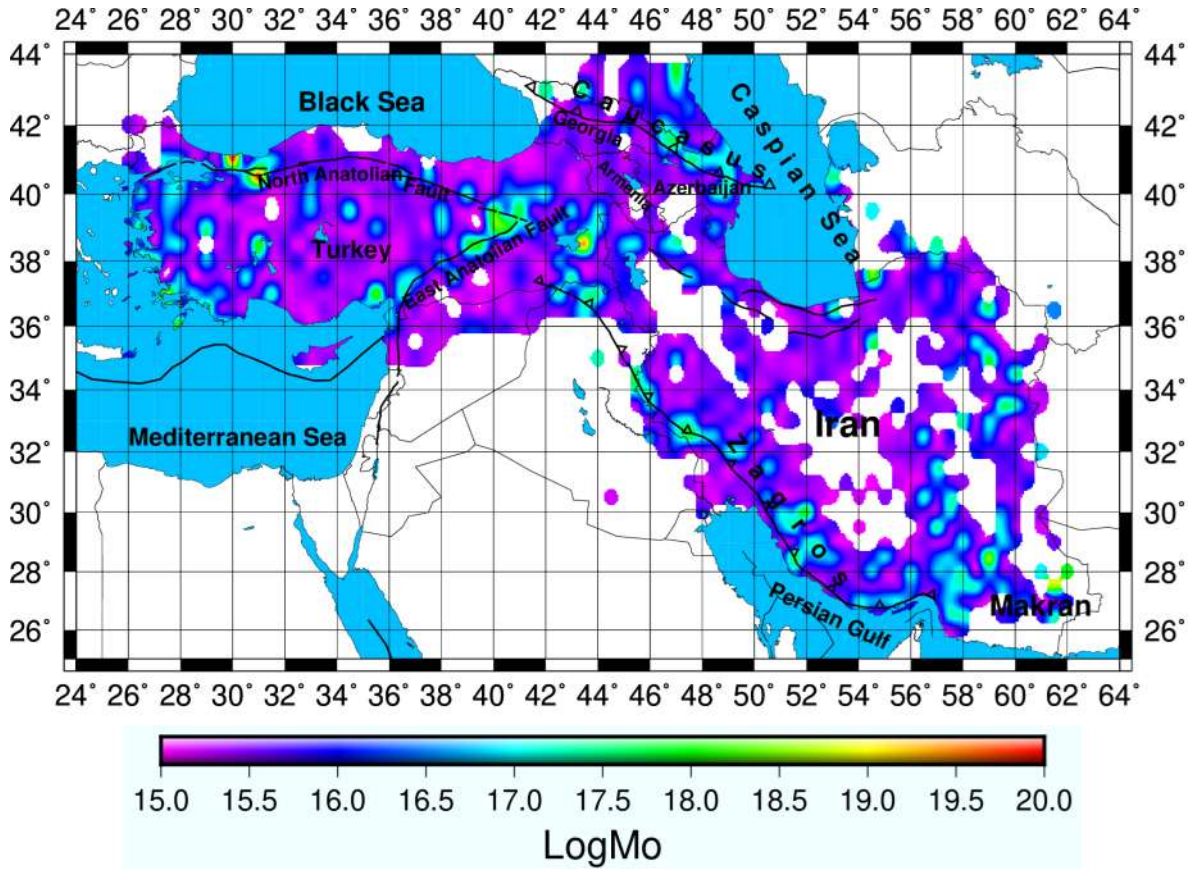

494

495 **Fig. 11** The map shows estimated moment release from the different catalogues from 1998 to
496 2020.

497

498

499

500

501

502

503

504

505

506

507

508 **Table 1**. Reported strong earthquakes in the research area.

Place	Date yy/mm/dd	Longitude (deg)	Latitude (deg)	Magnitude (Mw)	Depth (km)
Erzincan	1939/12/26	39.577	39.771	7.8	20
Gilan	1990/06/20	49.409	36.957	7.4	18.5
Erzincan	1992/03/13	39.605	39.710	6.7	27.2
Khorasan	1997/05/10	59.809	33.825	7.3	10
Izmit	1999/08/17	29.864	40.748	7.6	17
Düzce	1999/11/12	31.161	40.758	7.2	10
Baku	2000/11/25	49.946	40.245	6.2	50.4
Van	2011/10/23	43.508	39.721	7.1	18
Khash	2013/04/16	61.996	28.033	7.7	80
Kermanshah	2017/11/12	45.959	34.911	7.3	19
Elazığ	2020/01/24	39.061	38.431	6.7	10

509

Figures

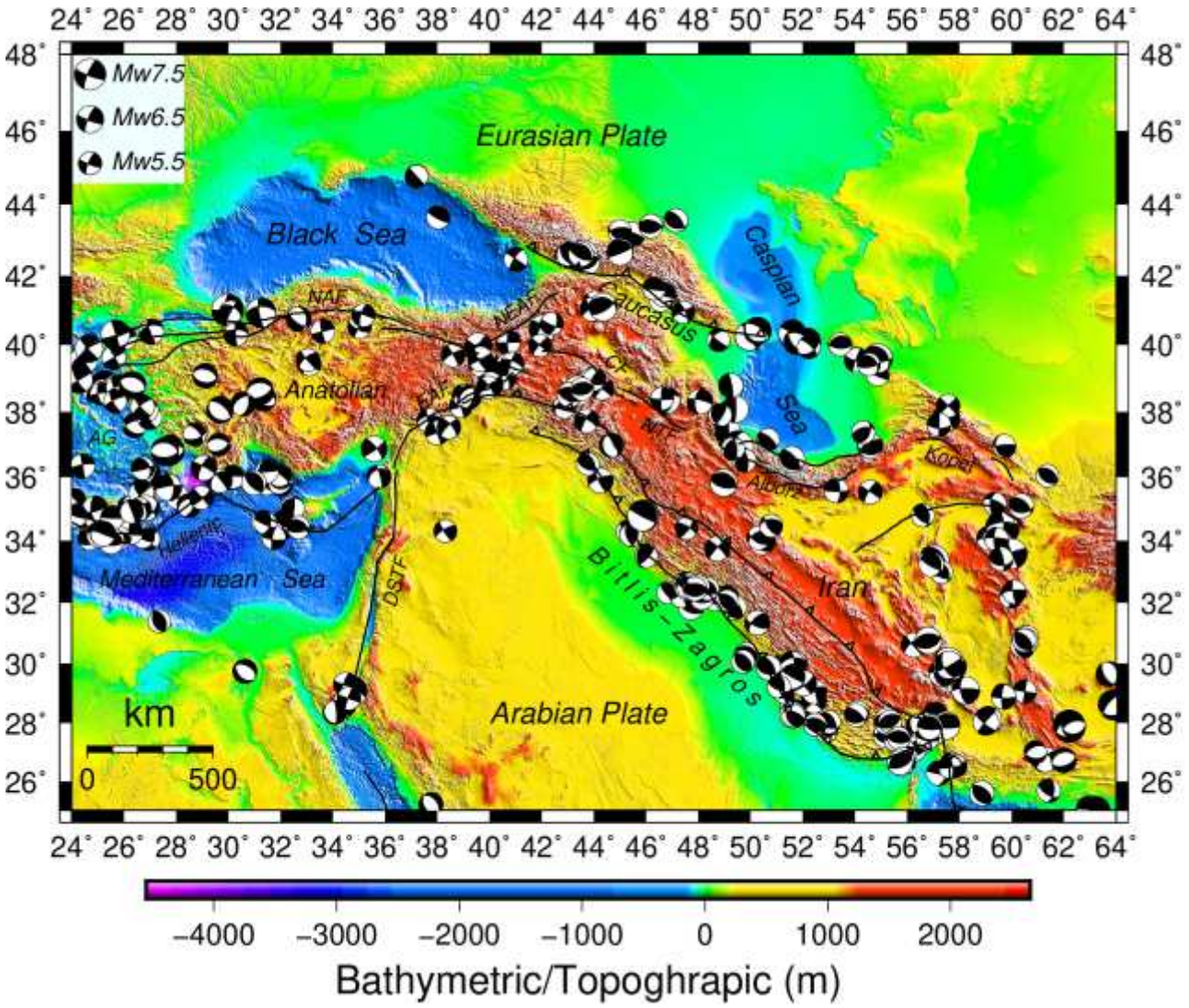

Figure 1

Tectonic and topographic/bathymetric map (SRTM30 plus) of the research area, including the interplay zone of the Eurasian, Arabian and Nubia plates. Abbreviations: AG (Aegean), NAF (North Anatolian Fault), EAF (East Anatolian Fault), DSTF (Dead Sea Transform Fault), NEAF (North-East Anatolian Fault), CF (Chalderan Fault), NTF (North Tabriz Fault). Black beach balls represent the focal mechanism of the earthquakes (M_w≥5.5, 1976-2020) from global Centroid Moment Tensor CMT). Note: The designations employed and the presentation of the material on this map do not imply the expression of any opinion whatsoever on the part of Research Square concerning the legal status of any country, territory, city or area or of its authorities, or concerning the delimitation of its frontiers or boundaries. This map has been provided by the authors.

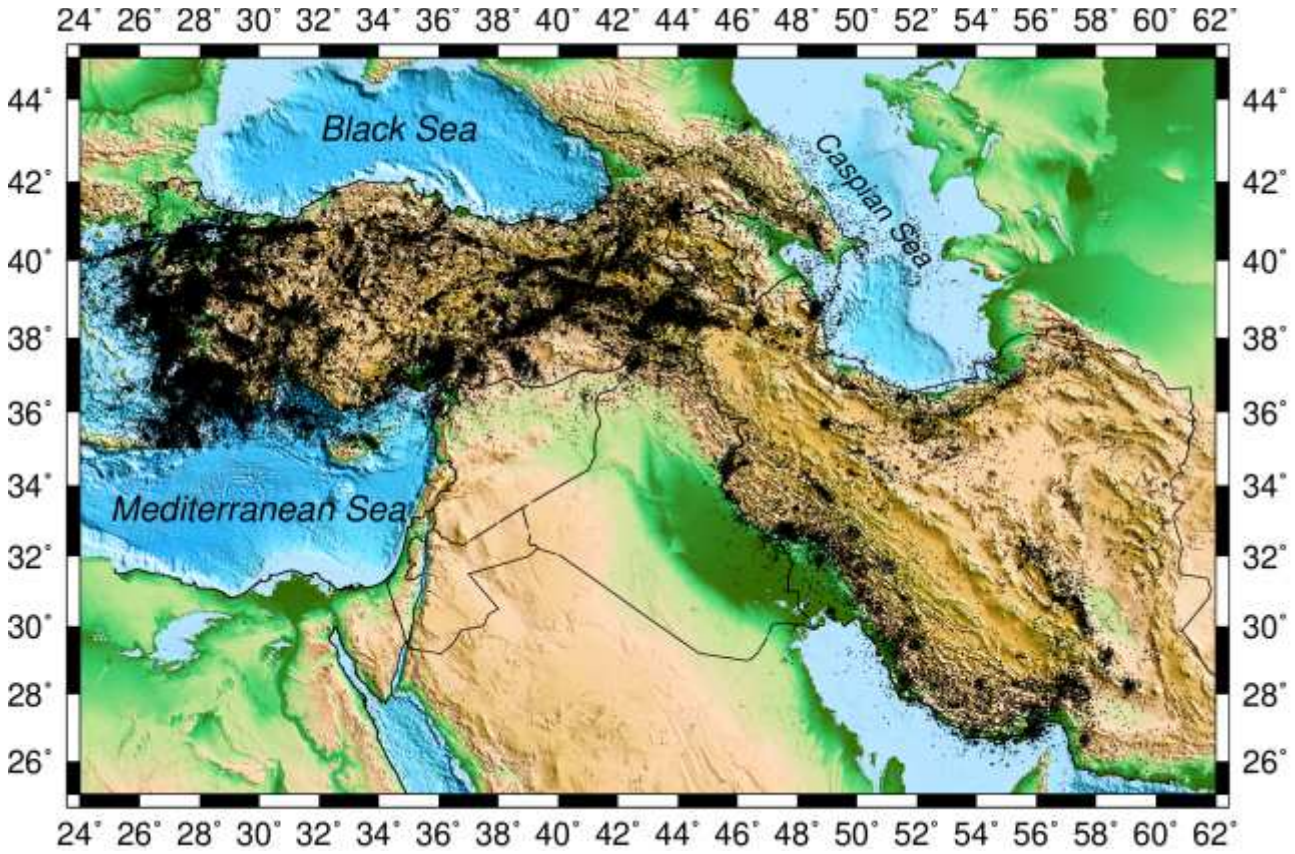

Figure 2

The map represents the distribution of the earthquakes in the study region (1998-2020). Note: The designations employed and the presentation of the material on this map do not imply the expression of any opinion whatsoever on the part of Research Square concerning the legal status of any country, territory, city or area or of its authorities, or concerning the delimitation of its frontiers or boundaries. This map has been provided by the authors.

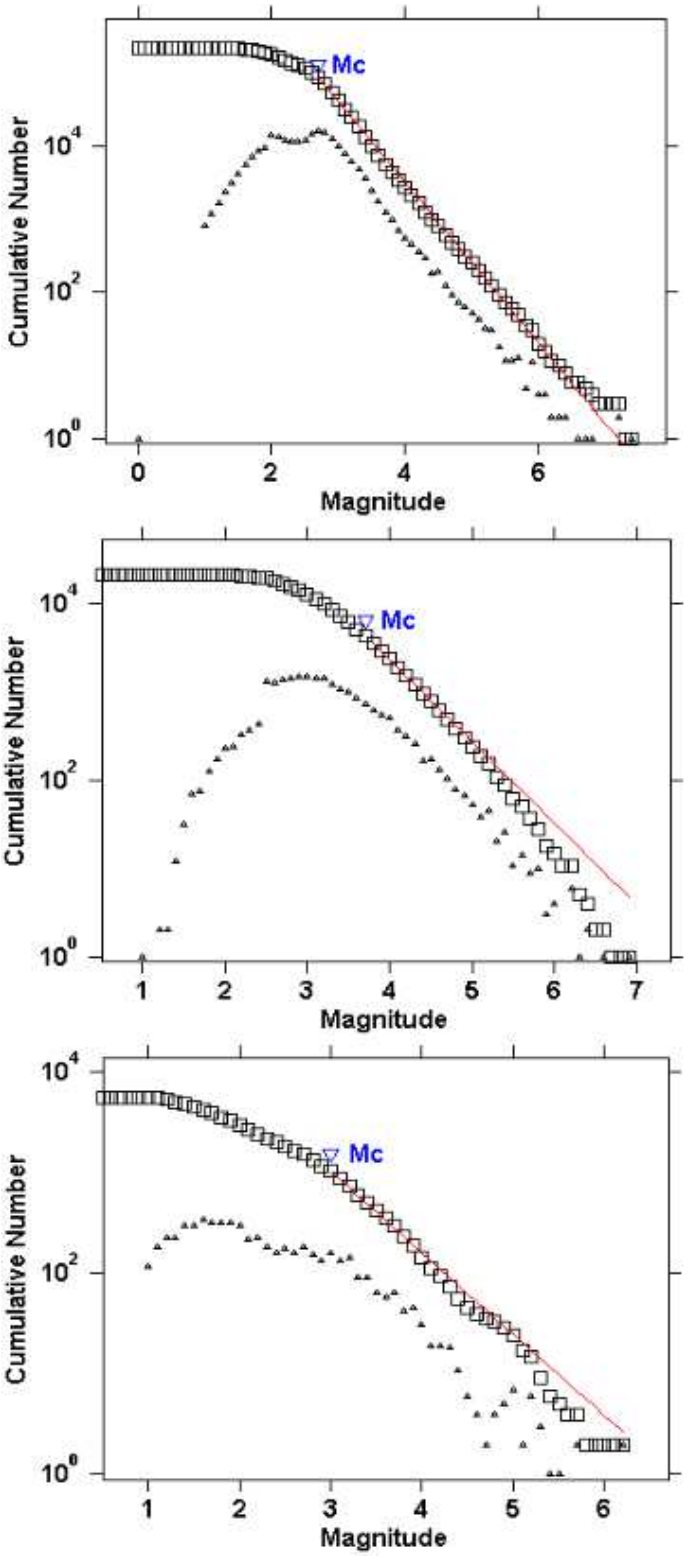

Figure 3

Frequency-magnitude number of earthquakes from. The solid line and triangle marked as best fit and magnitude of completeness.

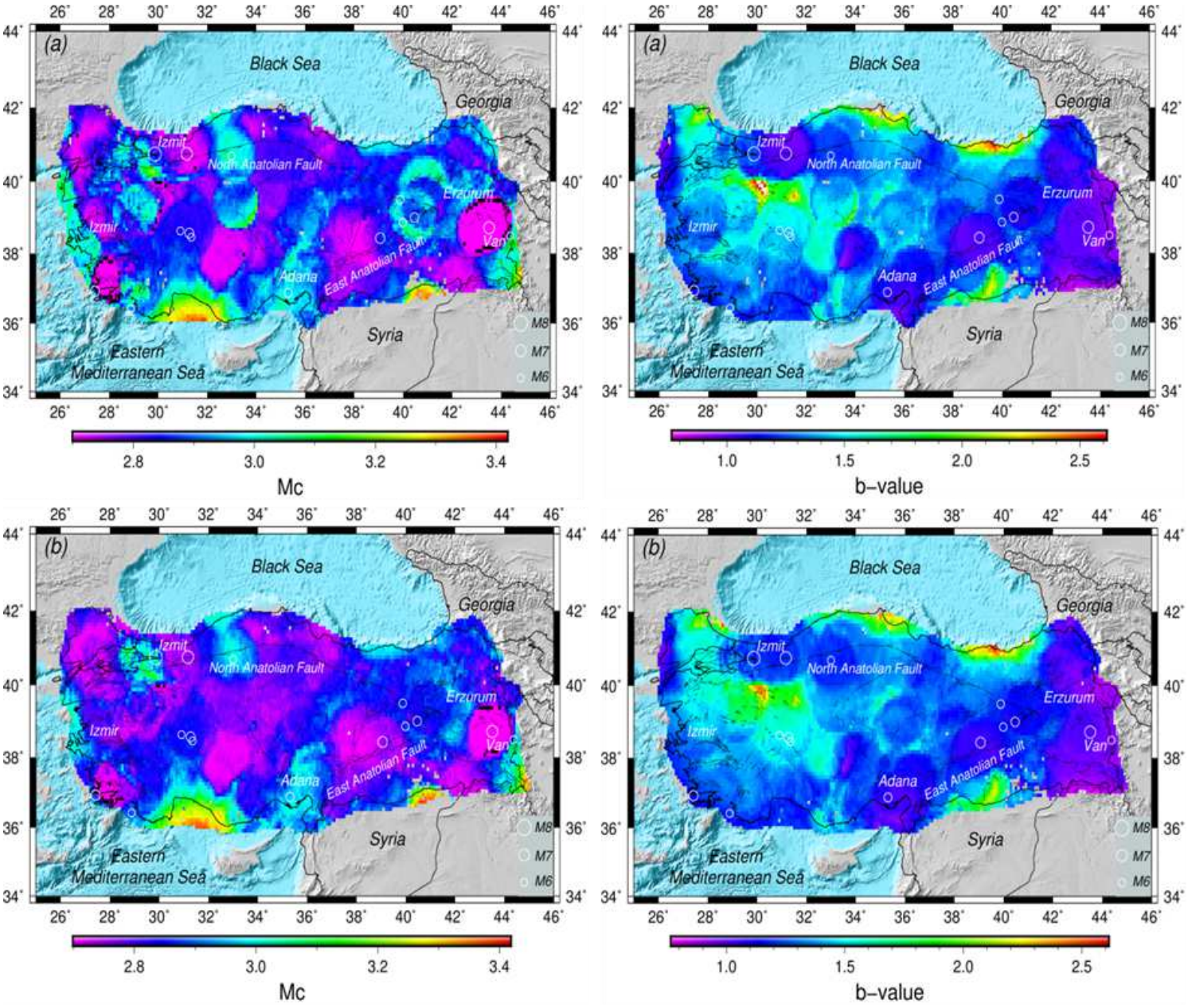

Figure 4

The maps of calculated b-value and Mc variations from non-declustered (upper) and declustered (bottom) catalogues for Turkey in the period of 1998-2020 from KOERI catalogue. Note: The designations employed and the presentation of the material on this map do not imply the expression of any opinion whatsoever on the part of Research Square concerning the legal status of any country, territory, city or area or of its authorities, or concerning the delimitation of its frontiers or boundaries. This map has been provided by the authors.

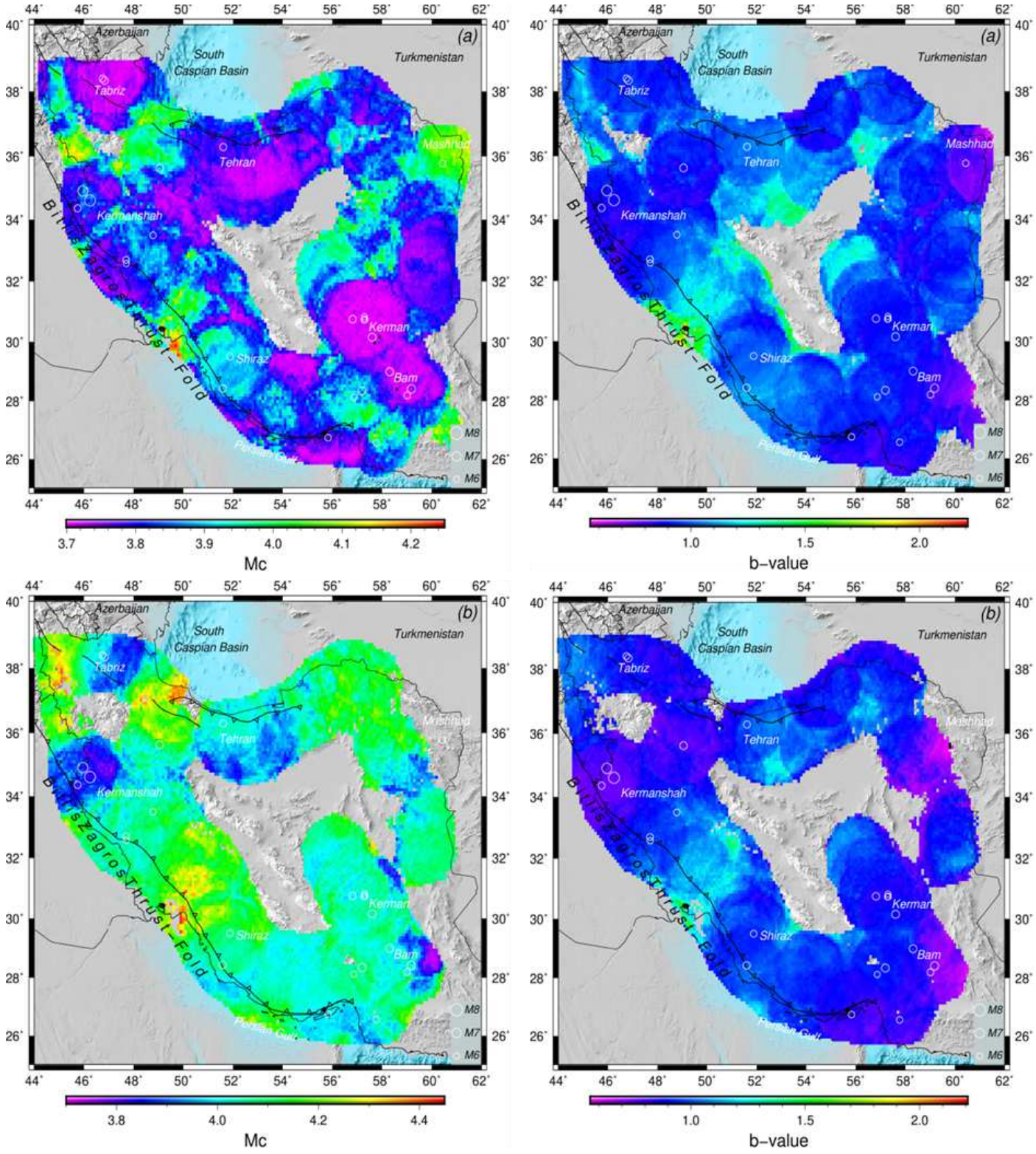

Figure 5

The maps of calculated b-value and Mc variations from non-declustered (upper) and declustered (bottom) catalogues in the period 1998-2020 for Iran using IIEES catalogue. Note: The designations employed and the presentation of the material on this map do not imply the expression of any opinion whatsoever on the part of Research Square concerning the legal status of any country, territory, city or

area or of its authorities, or concerning the delimitation of its frontiers or boundaries. This map has been provided by the authors.

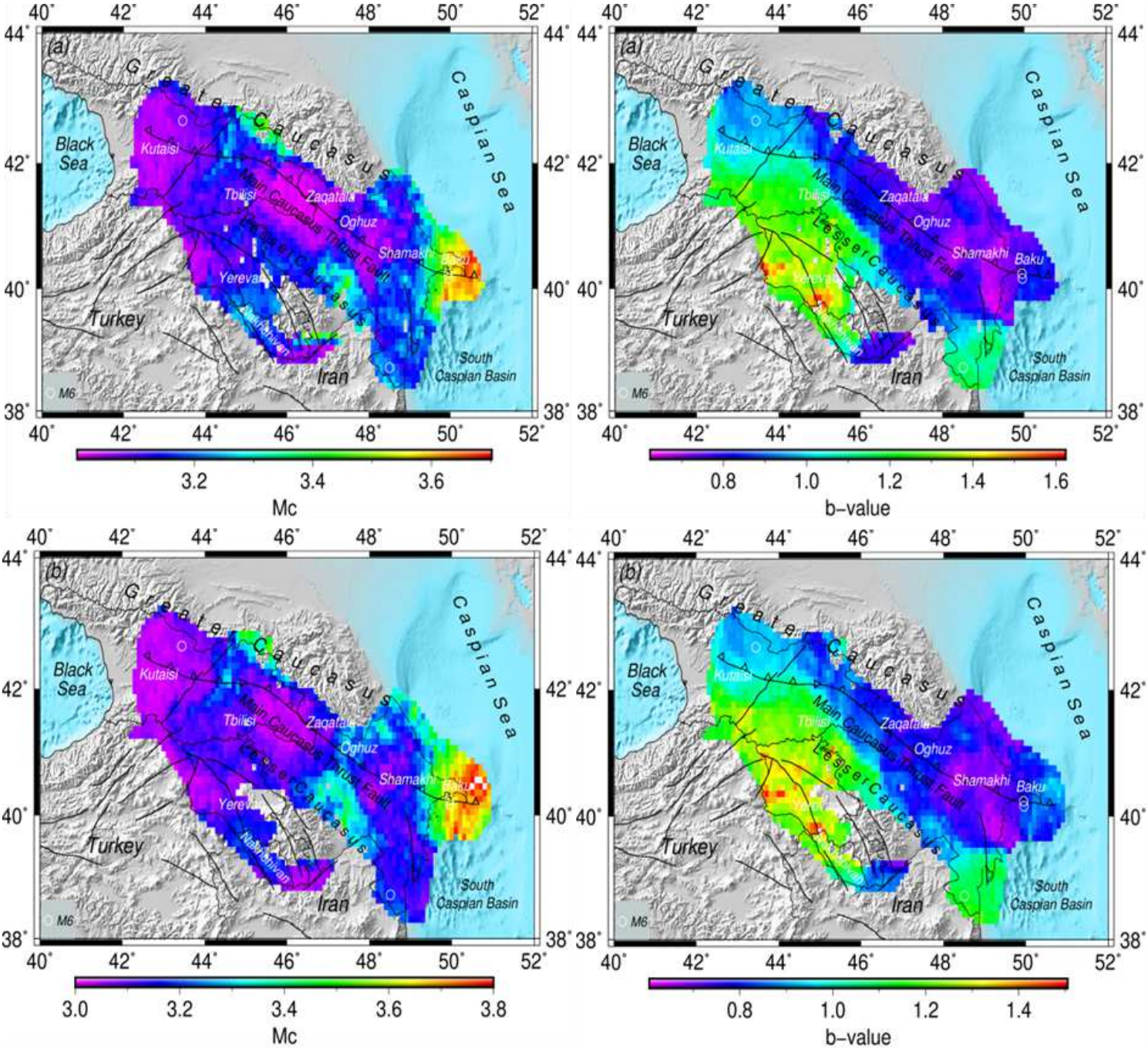

Figure 6

The maps of calculated b-value and Mc variations from non-declustered (upper) and declustered (bottom) catalogues in the period 1998-2020 in the Caucasus. Note: The designations employed and the presentation of the material on this map do not imply the expression of any opinion whatsoever on the part of Research Square concerning the legal status of any country, territory, city or area or of its authorities, or concerning the delimitation of its frontiers or boundaries. This map has been provided by the authors.

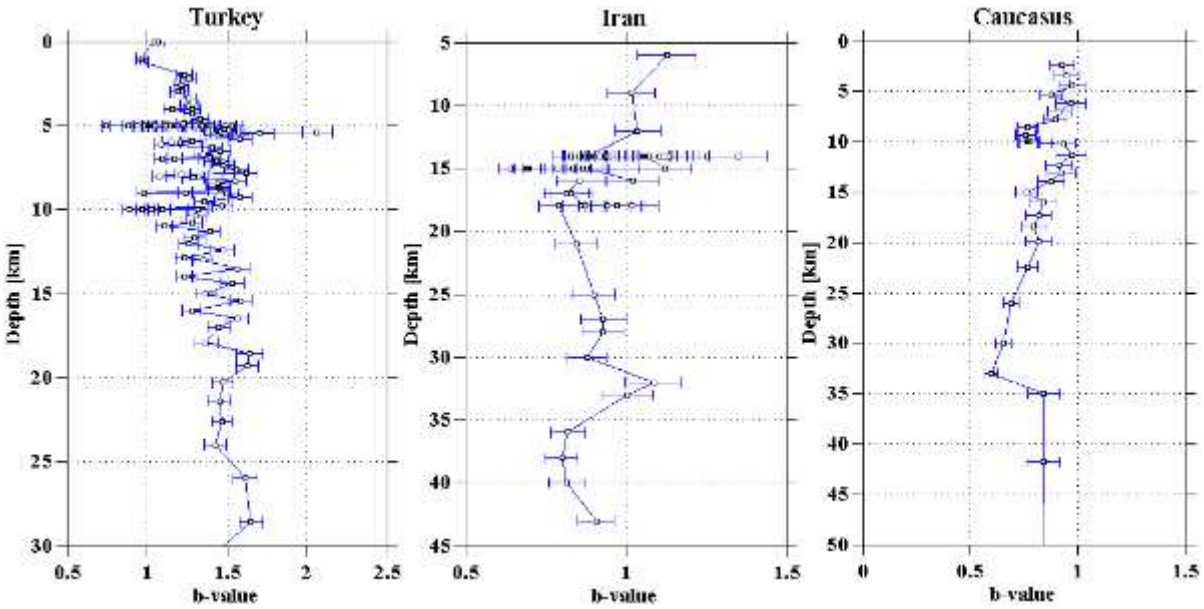

Figure 7

The map shows the calculated value of b and its error (horizontal bar) at a depth. Note: The designations employed and the presentation of the material on this map do not imply the expression of any opinion whatsoever on the part of Research Square concerning the legal status of any country, territory, city or area or of its authorities, or concerning the delimitation of its frontiers or boundaries. This map has been provided by the authors.

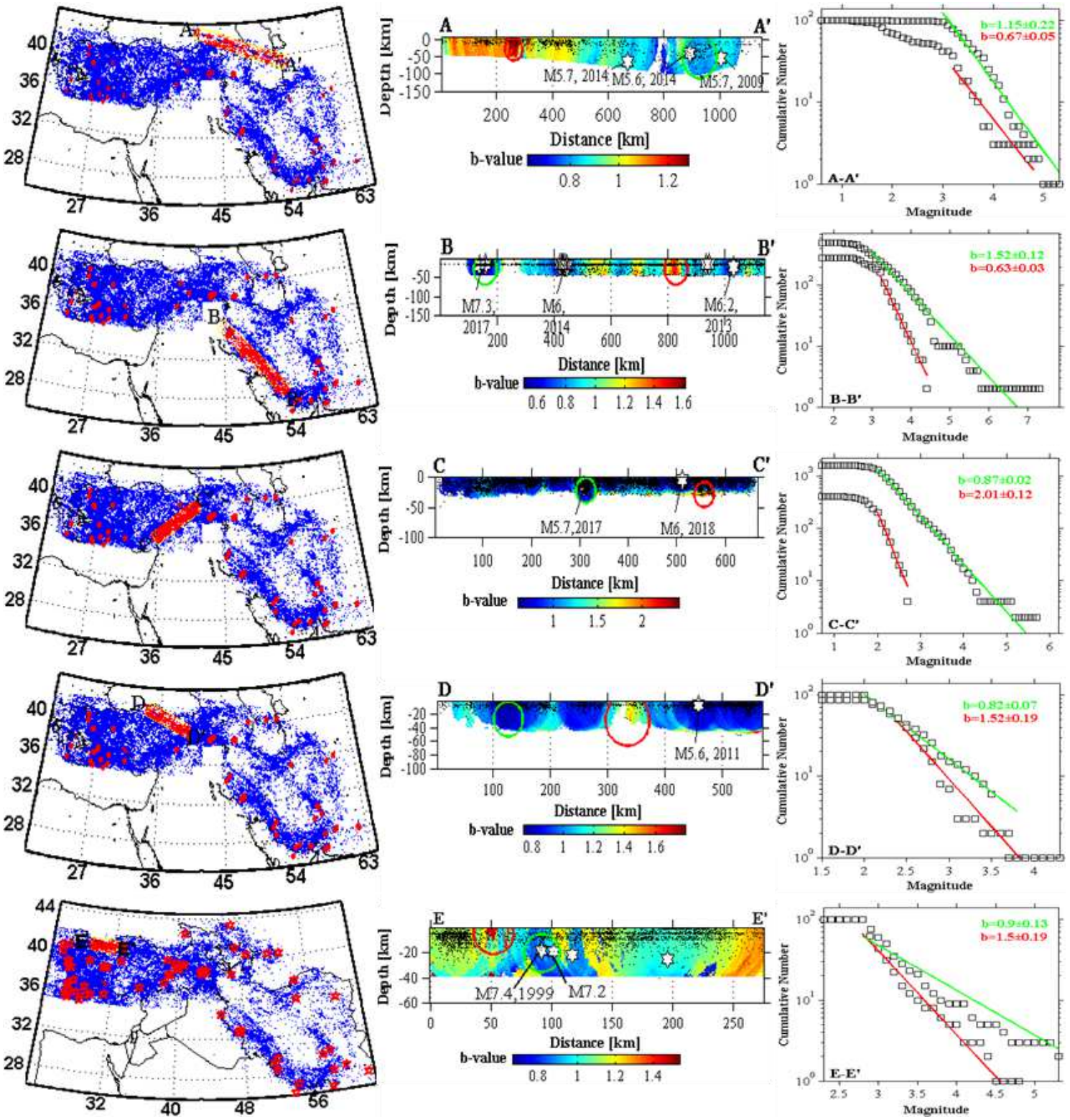

Figure 8

Vertical mapping of b-values. The left line shows the intersections. In the middle line, a b-value of 150 km is given around each section. In the right line, the pattern of b-value is presented. Note: The designations employed and the presentation of the material on this map do not imply the expression of any opinion whatsoever on the part of Research Square concerning the legal status of any country, territory, city or

area or of its authorities, or concerning the delimitation of its frontiers or boundaries. This map has been provided by the authors.

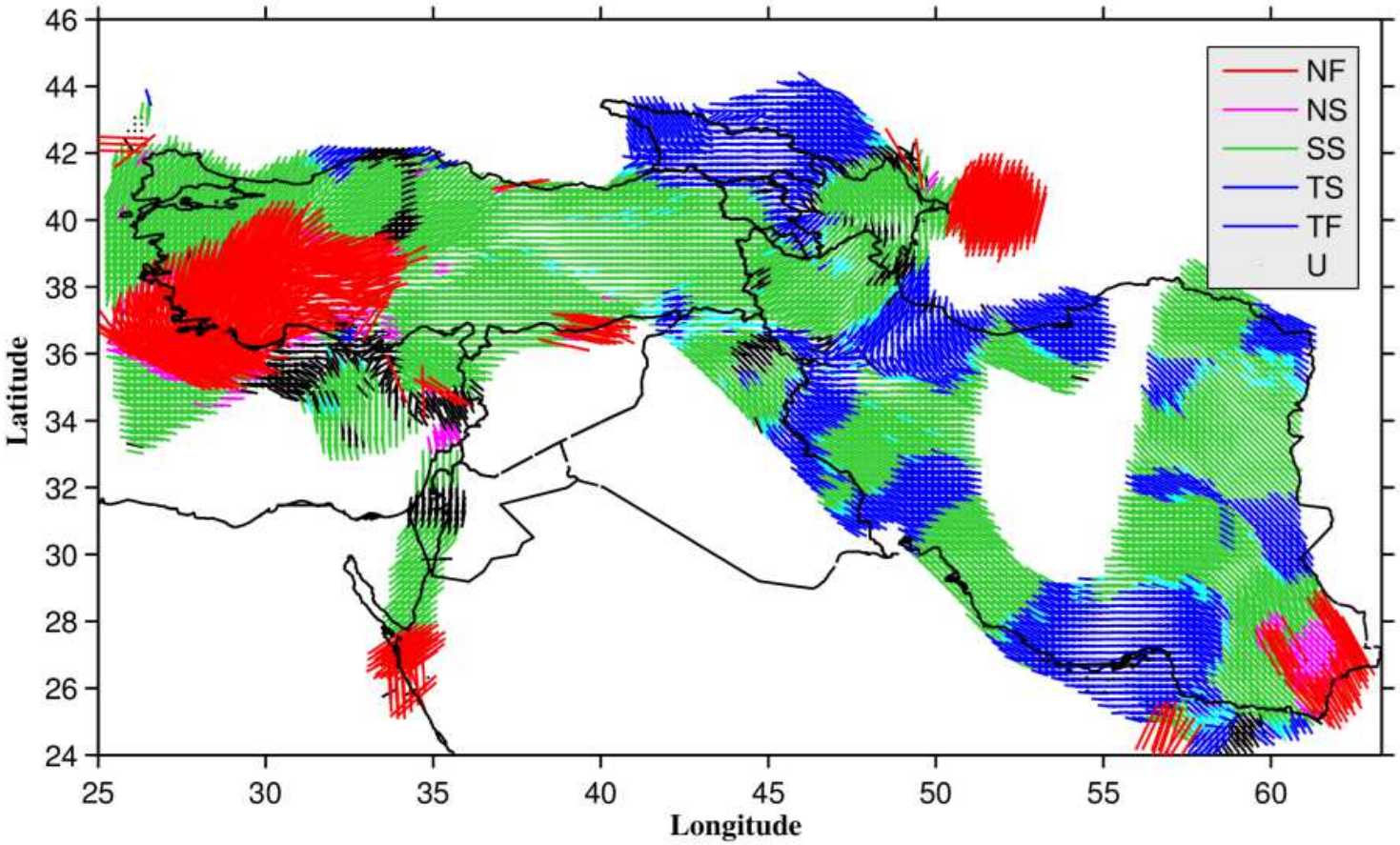

Figure 9

The direction of horizontal compression, different colors symbolize tectonic modes. (NF: Normal, NS: Normal with strike-slip, SS: Strike-slip, TS: Thrust with strike-slip, TF: Thrust). Note: The designations employed and the presentation of the material on this map do not imply the expression of any opinion whatsoever on the part of Research Square concerning the legal status of any country, territory, city or area or of its authorities, or concerning the delimitation of its frontiers or boundaries. This map has been provided by the authors.

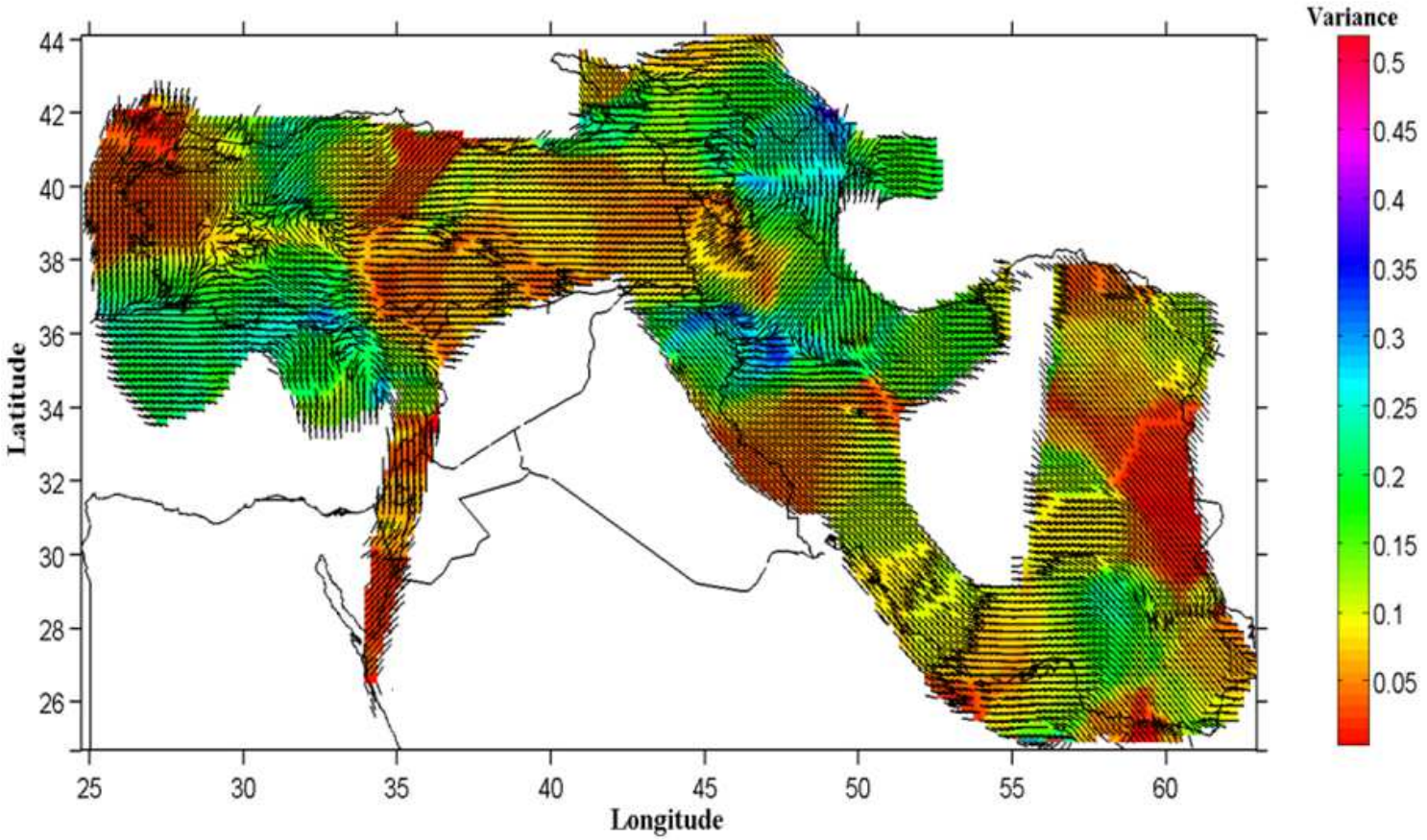

Figure 10

Horizontal compression orientation covered colored stress tensor variance map. Note: The designations employed and the presentation of the material on this map do not imply the expression of any opinion whatsoever on the part of Research Square concerning the legal status of any country, territory, city or area or of its authorities, or concerning the delimitation of its frontiers or boundaries. This map has been provided by the authors.

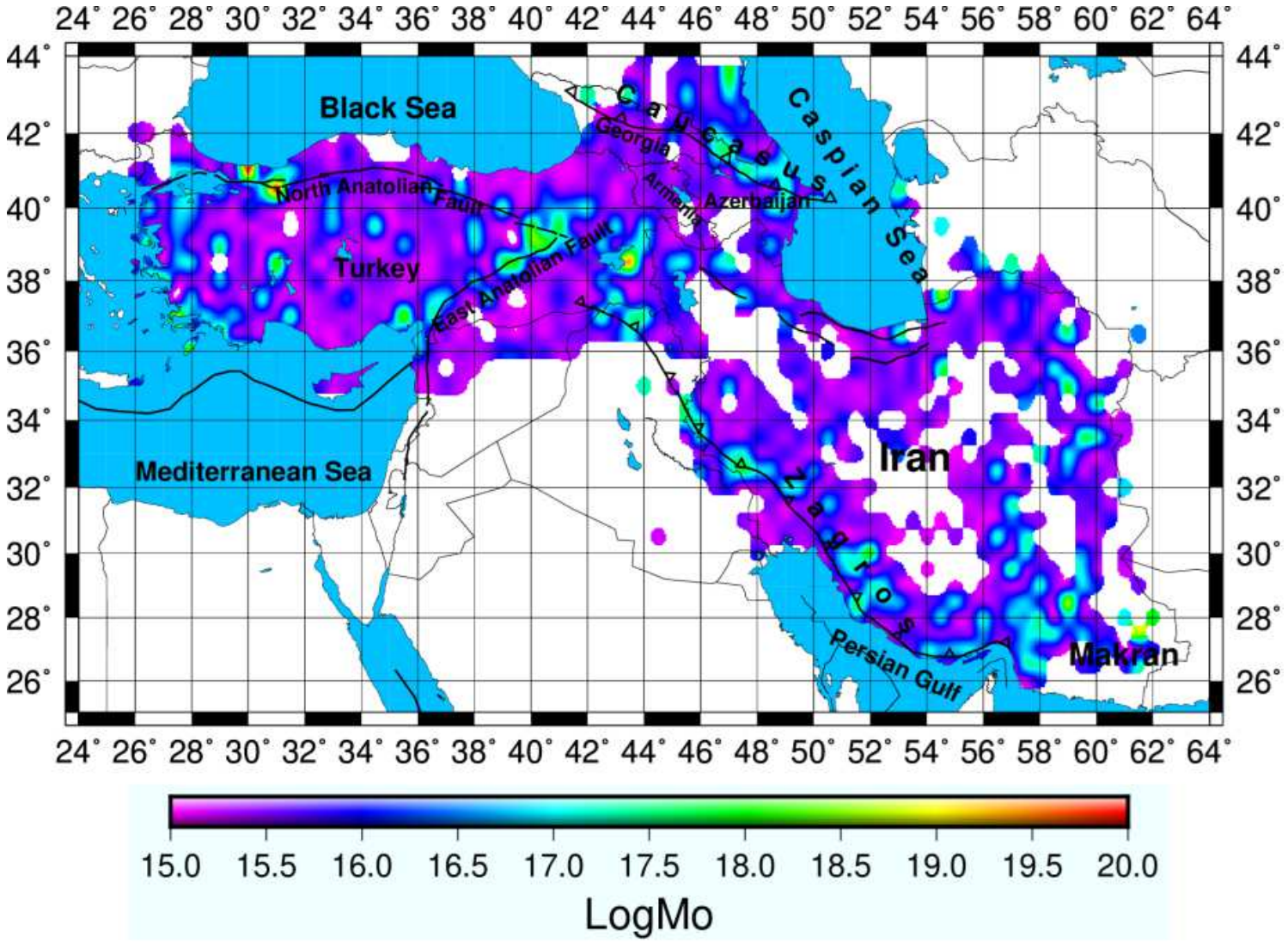

Figure 11

The map shows estimated moment release from the different catalogues from 1998 to 2020. Note: The designations employed and the presentation of the material on this map do not imply the expression of any opinion whatsoever on the part of Research Square concerning the legal status of any country, territory, city or area or of its authorities, or concerning the delimitation of its frontiers or boundaries. This map has been provided by the authors.